Ore Geology Reviews 151 (2022) 105219

Contents lists available at ScienceDirect

Ore Geology Reviews

journal homepage: www.elsevier.com/locate/oregeorev

Titanite geochemistry and its indicators for Cu-mineralized magmas: Insight from three dioritic intrusions in the Tongling area of the Lower Yangtze River metallogenic belt

Li-Chuan Pan [a], Rui-Zhong Hu [a,b,*], Qian Liu [a,b], Jin-Wei Li [a], Jin-Xiang Li [a]

[a] State Key Laboratory of Ore Deposit Geochemistry, Institute of Geochemistry, Chinese Academy of Sciences, Guiyang 550081, China
[b] College of Earth and Planetary Sciences, University of Chinese Academy of Sciences, Beijing 100049, China

ARTICLE INFO

Keywords:
Titanite
Porphyry-skarn Cu deposit
Cu mineralization potential
Oxidation state
Tongling area

ABSTRACT

Titanite has been regarded as a potential petrogenetic and metallogenic indicator owing to its stability and enrichment of trace elements. To verify the availability of geochemical titanite proxies in the Cu-mineralized magma system and to reveal magmatic constraints on Cu mineralization related to magmatic hydrothermal fluid, in situ major and trace element abundances and Nd isotopes of igneous titanite were determined for three Mesozoic diorite intrusions in the Tongling ore district of eastern China. The investigated intrusions were the Tongguanshan, Fenghuangshan, and Hucun intrusions, all of which host porphyry-skarn Cu deposits. Our study shows that the titanite δEu value and Fe/Al ratio, rather than the δCe and Ga content, are more effective indicators of the magma oxidation state in all three intrusions. Based on the titanite δEu value and Fe/Al ratio, the causative magma of the Fenghuangshan intrusion (titanite δEu = 0.50 ± 0.08; Fe/Al = 0.21 ± 0.07) was identified as being less oxidized than those of the Tongguanshan (titanite δEu = 0.64 ± 0.09; Fe/Al = 0.93 ± 0.15) and Hucun (titanite δEu = 0.80 ± 0.03; Fe/Al = 0.91 ± 0.04) intrusions. This result was consistent with the zircon Ce^{4+}/Ce^{3+} ratio. Moreover, owing to the limited effect of fluid exsolution and fractional crystallization on the F content of the investigated titanite, the higher titanite F content of the Fenghuangshan intrusion (titanite F = 0.40 ± 0.09 wt%) implies that the parental magma of this intrusion is more F-enriched than those of the Hucun (titanite F = 0.17 ± 0.09 wt%) and Tongguanshan (titanite F = 0.10 ± 0.07 wt%) intrusions; however, titanites from all three Cu-mineralized intrusions had similar or lower F content than those from intrusions without Cu mineralization. The above findings indicate that magmas with high oxygen fugacity have relatively high potential for porphyry-skarn Cu mineralization, while the high enrichment of F is not necessary for Cu mineralization. Additionally, we found that titanite $\varepsilon_{Nd}(t)$ values can inherit whole-rock $\varepsilon_{Nd}(t)$ values and thus can be used to investigate petrogenesis. This study confirms that titanite geochemistry is an efficient petrogenetic and metallogenic indicator for Cu-mineralized magma systems when the prerequisites are met.

1. Introduction

Porphyry-skarn Cu deposits, a main source of Cu resources, are recognized to have direct genetic links to oxidized and volatile (e.g., S, Cl, and H_2O)-rich intermediate-acid magmas (Mao et al., 2011; Peng et al., 2014; Zhao et al., 2015; Yang et al., 2020). However, the rocks associated with such mineralization usually undergo intense alterations (Lowell and Guilbert, 1970; Meinert et al., 2005), which may mask the true petrogenetic and metallogenetic processes (Cao et al., 2018) and dampen the effectiveness of using the chemical compositions of the whole rock and major rock-forming minerals that are susceptible to these alterations to investigate the magmatic oxidation state and volatile components. Titanite ($CaTiSiO_5$) is a common accessory mineral in intermediate-acid igneous rocks (Nakada, 1991; Bachmann et al., 2005; Glazner et al., 2008). Although titanite can potentially recrystallize during metamorphism (Scibiorski et al., 2019), it is usually better retained than the major rock-forming minerals, such as feldspar, biotite, and amphibole. Titanite is generally enriched in trace and halogen elements (Tiepolo et al., 2002; Buick et al., 2007; Hayden et al., 2008), the variations of which are strictly controlled by the physical and chemical magmatic nature (Xu et al., 2015). Therefore, when igneous titanite is unaltered, it can be a potential petrogenetic indicator for parental

* Corresponding author at: State Key Laboratory of Ore Deposit Geochemistry, Institute of Geochemistry, Chinese Academy of Sciences, Guiyang 550081, China.
E-mail address: huruizhong@vip.gyig.ac.cn (R.-Z. Hu).

https://doi.org/10.1016/j.oregeorev.2022.105219
Received 4 August 2022; Received in revised form 13 October 2022; Accepted 21 November 2022
Available online 22 November 2022

magma.

Previous studies have revealed that the oxidation state of the magma can largely determine its titanite Ga content and δEu and δCe values (King et al., 2013; Xu et al., 2015). The titanite Sn, W, Mo, and F concentrations can reflect magmatic metal fertility and volatile components (Aleksandrov and Troneva, 2007; Xie et al., 2010; Che et al., 2013; Wang et al., 2013; Pan et al., 2018). Zirconium in titanite can be used to estimate the magmatic temperature during titanite crystallization (Hayden et al., 2008); however, caution is required when using geochemical titanite proxies to trace specific magmatic information, as there may be multiple factors causing changes in the index values. For example, the oxidation state of the magma and the occurrence of feldspar crystallization can influence the titanite δEu value (Xu et al., 2015), meaning that when δEu is used to investigate the magma oxidation state, the effect of feldspar crystallization should be excluded to the greatest extent to avoid obtaining erroneous results. Hence, although the usability of geochemical titanite proxies has already been established, the preconditions for their use need to be further clarified.

To verify the availability of geochemical titanite proxies in Cu-mineralized magma systems and reveal constraints on magmatic

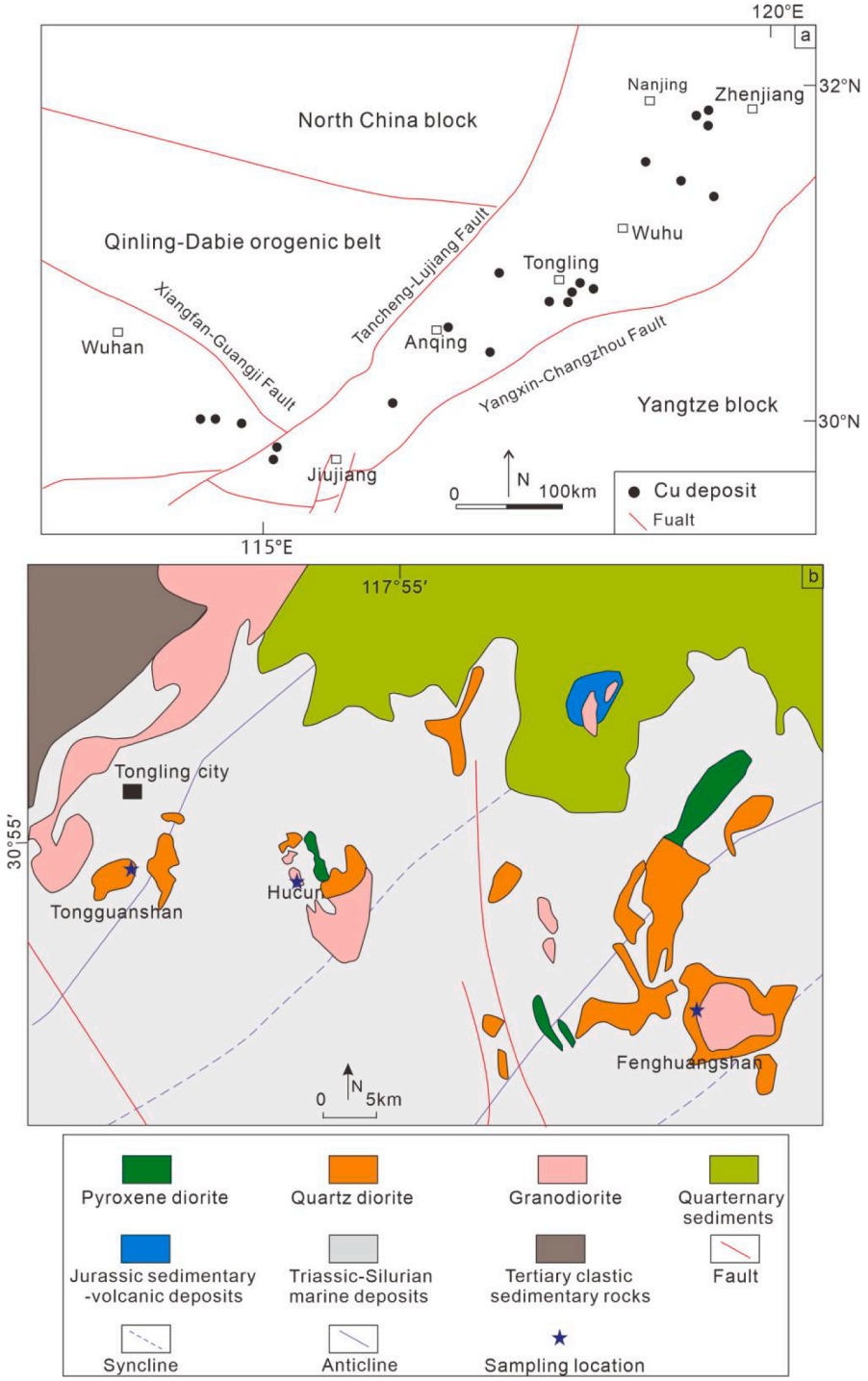

Fig. 1. Geological sketch map of the Lower Yangtze River metallogenic belt (a), modified from Liu et al. (2019) and Jiang et al. (2020); and the distribution of main igneous rocks in the Tongling ore district (b), modified from Liu et al. (2019) and Wang et al. (2022).

hydrothermal Cu mineralization, we investigated three typical dioritic intrusions hosting porphyry-skarn Cu deposits, namely Tongguanshan, Fenghuangshan, and Hucun in the Tongling ore district of the Lower Yangtze River metallogenic belt. The three intrusions were selected because titanite is widespread and not substantially altered, and because the genetic link between the intrusions and Cu deposits has previously been confirmed (Li et al., 2014; Cao et al., 2017; Wang et al., 2018; Jiang et al., 2020). The in situ elemental and Nd isotopic compositions of igneous titanite were analyzed using electron probe X-ray micro-analysis, laser ablation-inductively coupled plasma-mass spectrometry (LA-ICP-MS), and laser ablation multicollector inductively coupled plasma-mass spectrometry. A series of suitable geochemical titanite proxies were then selected to explore the magmatic information related to porphyry-skarn Cu mineralization. This study potentially provides new evidence of how titanite could be used as an ore exploration tool.

2. Geological background and sample descriptions

The Lower Yangtze River metallogenic belt is located in the northern margin of the Yangtze Block, separated from the Jiangnan orogenic belt by the Yangxing-Changzhou fault, and separated from the North China Craton and Dabie orogenic belt by the Tancheng-Lujiang and Xiangfan-Guangji faults (Fig. 1a). The Tongling area, famous for its numerous porphyry and skarn Cu deposits, is situated in the northeastern part of the Yangtze Block, close to the North China Block (Fig. 1a) (Liu and Peng, 2004; Yang et al., 2011). The regional metamorphic basement formed in the Precambrian and were covered by extensive Late Paleozoic marine carbonate rocks (Deng et al., 2011; Cao et al., 2017) that contributed to the Mesozoic skarn-type Cu mineralization (Chang et al., 1991; Pan and Dong, 1999). During the Middle Triassic, the Yangtze and North China blocks collided and caused intracontinental deformation (Xie et al., 2012). Magmatism related to Cu-Au-Pb-Zn mineralization occurred in the Late Jurassic and Early Cretaceous for the durations of 152–135 Ma and 135–124 Ma (Wang et al., 2022). The early-stage magmatism produced many dioritic intrusions associated with porphyry and skarn-type Cu and Au deposits and the late-stage magmatism produced various intermediate-acid intrusions associated with Pb-Zn deposits (Wang et al., 2022). It is thought that the Mesozoic magmatism and metallogenesis may have formed in an intra-continental tension setting without plate subduction (Xu et al., 2002; Wang et al., 2006; Wang et al., 2007; Yan et al., 2008). Alternatively, it may have been triggered by the subduction of the Paleo-Pacific slab to the west (Faure et al., 1996; Zhou and Li, 2000; Zhou et al., 2006; Li and Li, 2007; Sun et al., 2007). Geochronology has showed that the formation of Cu-mineralized intrusions was concentrated at approximately 140 Ma (Sun et al., 2003; Mao et al., 2006). These Cu-mineralized intrusions are mainly distributed in the Tongguanshan, Shizishan, and Fenghuangshan orefields. The typical representatives include the Tongguanshan, Hucun, and Fengshuoshan intrusions (Fig. 1b).

The 1.5-km^2 Tongguanshan intrusion, near Tongling City, is dominated by quartz diorite (Fig. 2a). Zircon U-Pb dating has identified that this intrusion was formed at approximately 137 Ma (Xu et al., 2005; Jiang et al., 2020). Several porphyry-skarn Cu ore bodies occur in the interior and periphery of this intrusion, and three types of Cu mineralization, that is, skarn, layered, and quartz-vein, were identified. The direct genetic relationship between the Tongguanshan quartz diorite and Cu deposits has been partially confirmed by the H, O, C, S, and Si isotopic compositions of rocks and ore minerals (Tian et al., 2005). The

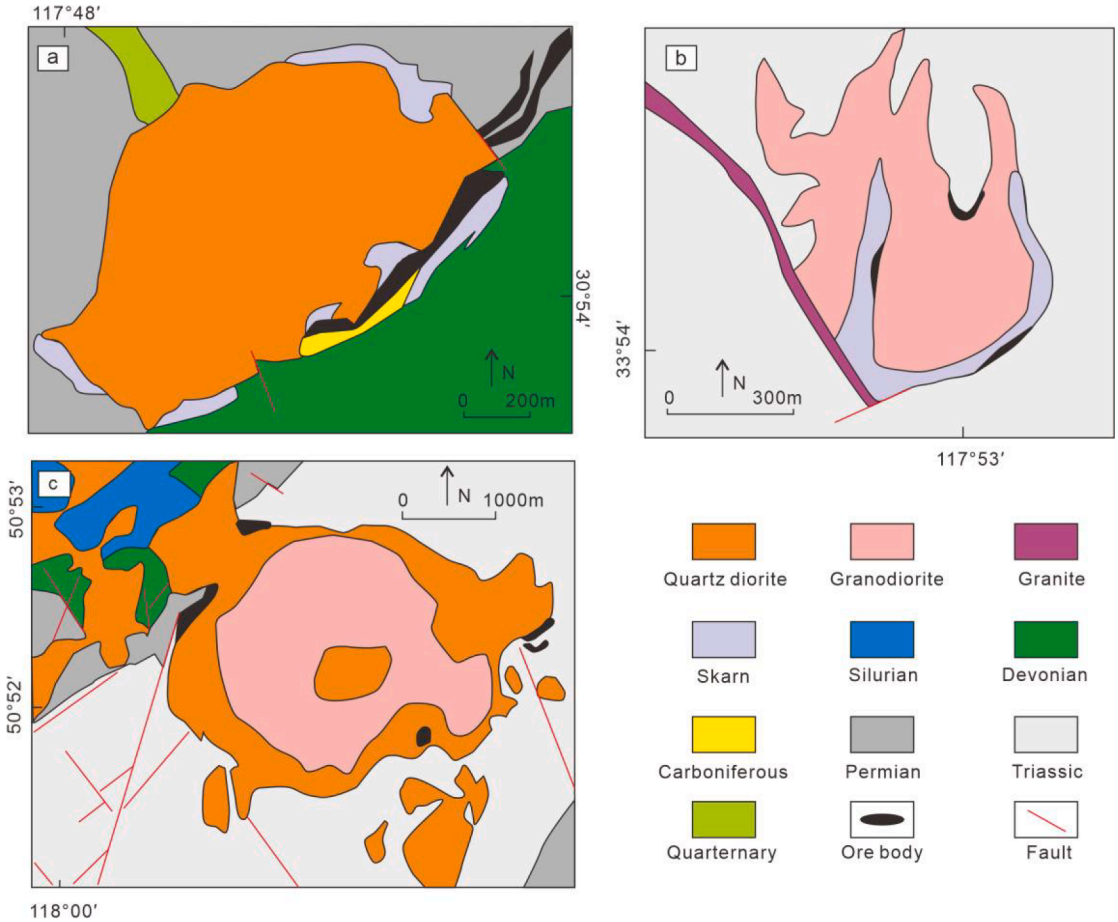

Fig. 2. Simplified geological map of the Tongguanmshan (a), Hucun (b), and Fenghuangshan (c) intrusions, modified from Jiang et al. (2020), Xie et al. (2020), and Zheng et al. (2015), respectively.

selected quartz diorite samples of the Tongguanshan intrusion are gray in color and contain plagioclase (~55 vol%), K-feldspar(~15 vol%), quartz (~15 vol%), amphibole (~10 vol%), and biotite (~5 vol%) as the major mineral phases and apatite, titanite, and zircon as accessory mineral phases. Titanite usually coexists with plagioclase, amphibole, and quartz (Fig. 3 a–c).

The 0.35-km^2 Hucun intrusion, 7 km east of Tongling City, is composed of granodiorite (Fig. 2b). Zircon U-Pb dating has identified the formation of this intrusion as occurring at 140.0 ± 2.6 Ma (Xu et al., 2008). Two types of Cu mineralization are present in the Hucun Cu deposit, that is, porphyry mineralization in the interior of the intrusion and skarn mineralization in the contact zone between the intrusion and carbonate wall rock. The Pb and S isotopic compositions of pyrite, as well as the C—H—O isotopic compositions of fluid inclusions, indicate that the metallogenic materials came primarily from the causative granodiorite magma (Lu et al., 2007; Cao et al., 2017; Shi et al., 2020). The selected granodiorite samples of the Huncu intrusion are light-gray in color and primarily consist of plagioclase (~40 vol%), quartz (~25 vol%), K-feldspar (~15 vol%), amphibole (~15 vol%), and biotite (~5 vol%), with apatite, zircon, and titanite as accessory minerals. Titanite usually coexists with plagioclase and quartz (Fig. 3 d–f).

The Fenghuangshan intrusion, also known as the Xinwuli intrusion, is situated approximately 35 km southeast of Tongling City, and is the largest diorite intrusion in the Tongling ore district, covering approximately 10 km^2. This intrusion consists of quartz diorite and granodiorite (Fig. 2c). Both skarn- and porphyry-type Cu mineralization developed in the Fenghuangshan Cu deposit. The consistency between its zircon U-Pb ages (143.1 ± 1.6 Ma) and molybdenite re-Os ages (141.71 ± 0.82 Ma) suggests the simultaneous formation of the Cu deposit and the Fenghuangshan granodiorite (Li et al., 2014). The C—O—S isotopes of hydrothermal calcite and sulfides have revealed the magmatic origin of hydrothermal fluid, implying a potential genetic relationship between the Cu deposit and that intrusion (Wang et al., 2018). The selected granodiorite samples of the Fenghuangshan in this study are gray in color and are composed of plagioclase (~45 vol%), quartz (~25 vol%), K-feldspar (~15 vol%), amphibole (~10 vol%), and biotite (~5 vol%) as the main mineral phases and apatite, zircon, and titanite as accessory mineral phases. Titanite usually coexists with plagioclase, quartz, and biotite (Fig. 3 g–i).

3. Analytical methods

Seven rock samples (two from Fenghuangshan, two from Hucun, and three from Tongguanshan) were obtained and prepared for whole-rock chemical analysis. One rock sample from each intrusion was used for titanite and zircon selection. The rock samples used in this study did not exhibit signs of serious alteration and weathering.

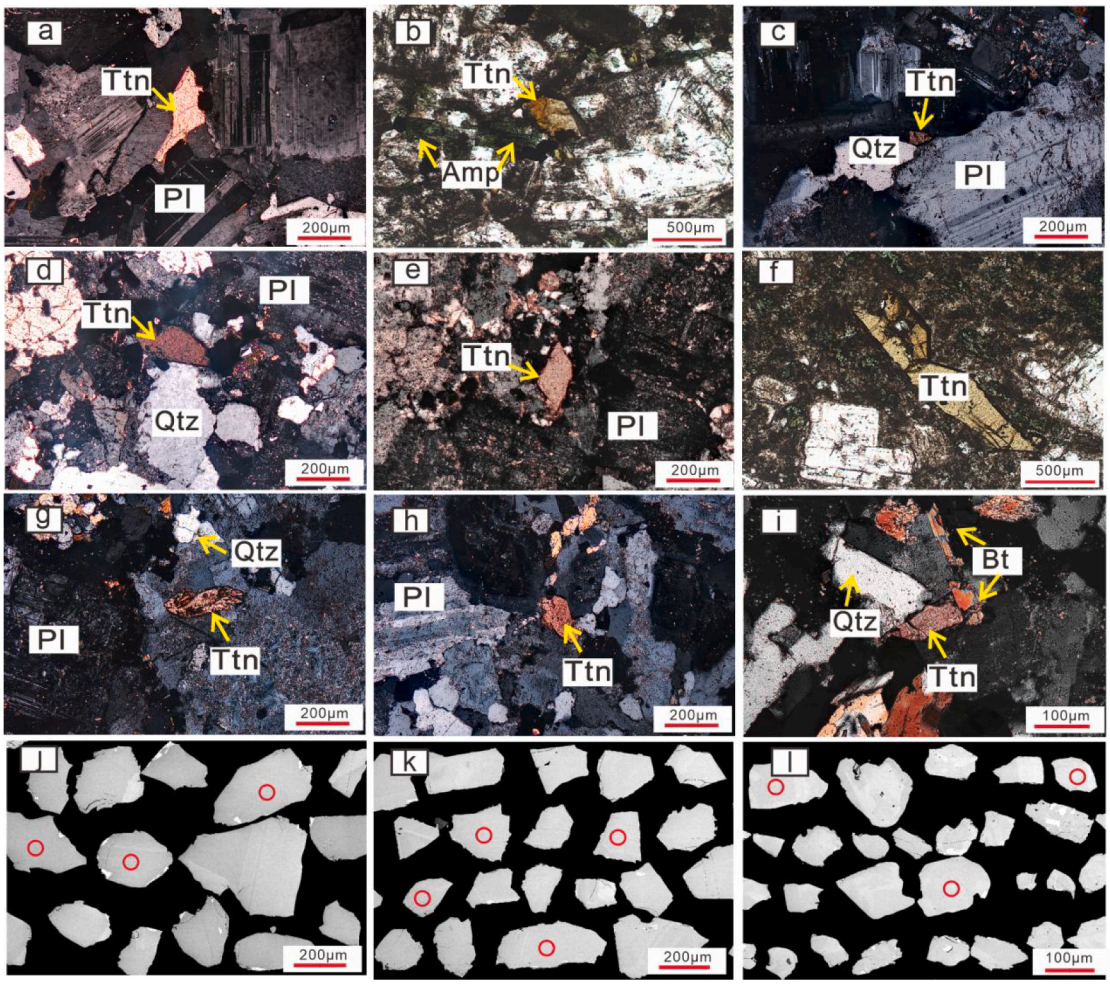

Fig. 3. Modes of the occurrence of titanite in the rock samples from the Tongguanshan (a–c), Hucun (d–f), and Fenghuangshan (g–i) intrusions and the backscattered electron images of titanite grains from Tongguanshan (j), Hucun (k), and Fenghuangshan (l). The red circles represent the analyzed points of titanite grains. Amp: amphibole, Bt: biotite, Pl: plagioclase, Qtz: quartz, Ttn: titanite. (For interpretation of the references to color in this figure legend, the reader is referred to the web version of this article.)

3.1. Whole-rock chemical analyses

The concentrations of the major elements in the selected rocks were determined with fused lithium tetraborate glass pellets using an ARL Perform'X 4200 X-ray fluorescence spectrometer at the State Key Laboratory of Ore Deposit Geochemistry, Institute of Geochemistry, Chinese Academy of Sciences in Guiyang (hereafter, SKLODG), with an analytical precision estimated as < 5 %. The concentrations of trace elements in the whole rocks were analyzed using a PlasmaQuant MS Elite ICP-MS at SKLODG. Powdered samples (50 mg) were dissolved in a mixture of HF and HNO_3 in high-pressure polytetrafluoroethylene vessels for 2 days at approximately 190 °C. Rh was used to monitor the signal drift during the analysis. The detailed analytical procedures have been described by Qi et al. (2000), and the analytical precision was estimated as within 10 %.

3.2. Titanite major and trace elements compositions analyses

Titanite crystals were separated from the samples using standard heavy liquid and magnetic methods and then mounted and polished in epoxy. Targets suitable for in situ analysis were chosen using back-scattered electron (BSE) images (Fig. 3 j–l). Since the regular zoning observed in the BSE images of titanite grains may be related to the variation of rare earth element (REE) content, indicating the magmatic evolution, and because the irregular zoning is interpreted as a result of fluid-assisted titanite recrystallization (Scibiorski et al., 2019), in order to obtain earlier magmatic information, the area near the core of titanite showing relatively homogenous brightness was preferentially analyzed.

The major and minor element contents in titanite were determined using a JXA8530F-plus electron microprobe at SKLODG. The analytical conditions were: 25 kV accelerating voltage, 10nA beam current, and 10 μm beam diameter. The following natural minerals were used for calibration: rutile (Ti), pyrope-garnet (Si, Al, Mg, Fe, and Mn), albite (Na), apatite (Ca and P), and phlogopite (F). The trace element contents in titanite were measured by in situ LA-ICP-MS at SKLODG. The LA-ICP-MS system was an Agilent 7700x ICP-MS equipped with a Resonetics RESOLution M-50 ArF-Excimer laser gun (λ = 193 nm, 80 mJ, and 10 Hz). The laser ablation spot had a diameter of 44 μm. The ablated aerosol was fed into the ICP instrument using He gas, and the NIST610 and NIST612 standards were used for calibration. Ca content of each grain was measured using ^{43}Ca and normalized using the concentration determined by electron probe analysis. Offline data reduction was performed using ICPMSDataCal software, following Liu et al. (2008).

3.3. Titanite Nd isotope composition analyses

The in situ titanite Nd isotope measurements were conducted using a Nu Plasma III MC-ICP-MS (Nu Instruments) attached to a RESOlution-155 ArF193-nm laser ablation system (Australian Scientific Instruments) at SKLODG. The titanite was ablated in a mixture of He (350 ml/min) and N_2 (2 ml/min) atmospheres with the following parameters: 30 s baseline time, 40 s ablation time, 60–104 μm spot size, 6 Hz repetition rate, and 6 J/cm^2 energy density. The interference of ^{144}Sm with ^{144}Nd was derived from the ^{147}Sm intensity with a natural $^{144}Sm/^{147}Sm$ ratio of 0.205484 (Isnard et al., 2005). The Sm mass bias factor was calculated from the measured isotopic ratio of $^{147}Sm/^{149}Sm$ and its accepted value of 1.08680 (Isnard et al., 2005). The mass bias of $^{143}Nd/^{144}Nd$ was normalized to $^{146}Nd/^{144}Nd = 0.7129$ using an exponential law. The standard "Durango apatite" was used after every-five samples, and AP2, another apatite standard, was used after every 30 unknown samples, as controls. The measured $^{143}Nd/^{144}Nd$ ratio for AP2 was 0.510999 ± 0.000017 (n = 4) and for Durango apatite was 0.512492 ± 0.000015 (n = 16), which matched the recommended values (AP2: 0.511007 ± 0.000030, Durango apatite: 0.512483 ± 0.000004) (Yang et al., 2014).

3.4. Zircon trace elements analyses

The contents of trace elements in zircon were analyzed by LA-ICP-MS at SKLODG using an Agilent 7900 ICP-MS equipped with a GeoLasPro 193 nm ArF excimer laser. A laser repetition of 6 Hz, an energy density of 3 J/cm2, and a spot size of 32 μm were used for this analysis, and the NIST610 and NIST612 standards were used for calibration. Offline data reduction was then performed using ICPMSDataCal software, following Liu et al. (2008).

4. Results

4.1. Whole-rock compositions

The major, minor, and trace elemental compositions of the rock samples from the selected intrusions (Hucun, Tongguanshan, and Fenghuangshan) are shown in Appendix 1. The data showed that all three intrusions are metaluminous and can be classified as high-K calc-alkaline series (Fig. 4a and b). In the chondrite-normalized REE diagram, all samples displayed fractionated REE patterns (Fig. 4c). There was little difference in the whole-rock δEu ($=Eu_N/(Sm_N \times Gd_N)^{(1/2)}$) (0.83–1.01) and δCe ($=Ce_N/(La_N \times Pr_N)^{(1/2)}$) (1.00–1.04) ratios among the three intrusions. All rock samples showed mild to strong Nb, Ta, P, and Ti depletion in primitive mantle-normalized trace-element patterns (Fig. 4d). Moreover, the three intrusions can be classified as adakite based on high $(La/Yb)_N$ ratio, unobvious negative Eu anomalies (Fig. 4c), high Sr/Y ratio, and low Y content (Fig. 5a).

4.2. Titanite major and trace elements

The major elemental composition of the sampled titanite is presented in Appendix 2. The CaO, TiO_2, and SiO_2 contents in titanites from the three selected intrusions showed limited variation (CaO: 26–28 wt%, TiO_2: 32–37 wt%, and SiO_2: 27–31 wt%). Titanites from the Fenghuangshan intrusion contained more F and Al_2O_3 (F: 0.40 ± 0.09 wt% and Al_2O_3: 1.60 ± 0.35 wt%) but less FeO (0.45 ± 0.10 wt%), and had a lower Fe/Al value (atoms per formula unit) (0.21 ± 0.07) than those from the Hucun (F: 0.17 ± 0.09 wt%; Al_2O_3: 1.16 ± 0.09 wt%, FeO: 1.50 ± 0.11 wt%, and Fe/Al: 0.91 ± 0.04) and Tongguanshan (F: 0.10 ± 0.07 wt%, Al_2O_3: 1.00 ± 0.11 wt%, FeO: 1.32 ± 0.23 wt%; Fe/Al: 0.93 ± 0.15) intrusions. Additionally, titanite from the Tongguanshan intrusion showed lower MnO (0.06 ± 0.04 wt%) than that from the Hucun (MnO: 0.14 ± 0.01 wt%) and Fenghuangshan intrusions (MnO: 0.17 ± 0.08 wt %).

The data from Appendix 2 indicate that titanite is rich in field strength elements (Ta: 16 ± 11.2 ppm to 127 ± 29.2 ppm; Zr: 475 ± 182 ppm to 606 ± 45.18 ppm; Hf: 25.33 ± 11.02 ppm to 37.80 ± 3.27 ppm; Th: 174 ± 147 ppm to 277 ± 47.9 ppm; U: 42.89 ± 3.27 ppm to 119.85 ± 129 ppm), REEs (7118 ± 2784 ppm to 15814 ± 1755 ppm), and other trace elements such as Sr (11.89 ± 2.04 ppm to 66.92 ± 3.24 ppm) and Ga (11.89 ± 2.04 ppm to 42.77 ± 5.11 ppm). The chondrite-normalized REE patterns of titanite showed enrichment in light REEs relative to heavy REEs, and were characterized by slightly negative Eu anomalies (0.50 ± 0.08 to 0.80 ± 0.03) and positive Ce anomalies (1.04 ± 0.07 to 1.17 ± 0.01) (Fig. 6).

4.3. Titanite Nd isotopes

The in situ Nd isotopic data of titanite are listed in Appendix 3. We chose the reliable zircon U-Pb ages obtained previously by SHRIMP (sensitive high-resolution ion microprobe) and LA-ICP-MS (Xu et al., 2005; Xu et al., 2008; Li et al., 2014) as the formation ages of the three intrusions, and calculated the titanite $\varepsilon_{Nd}(t)$ values of the selected intrusions. The average titanite $\varepsilon_{Nd}(t)$ values were −12.3 ± 1.3 in the Tongguanshan intrusion, −10.7 ± 1.5 in the Fenghuangshan intrusion, and −10.1 ± 0.7 in the Hucun intrusion (Fig. 7).

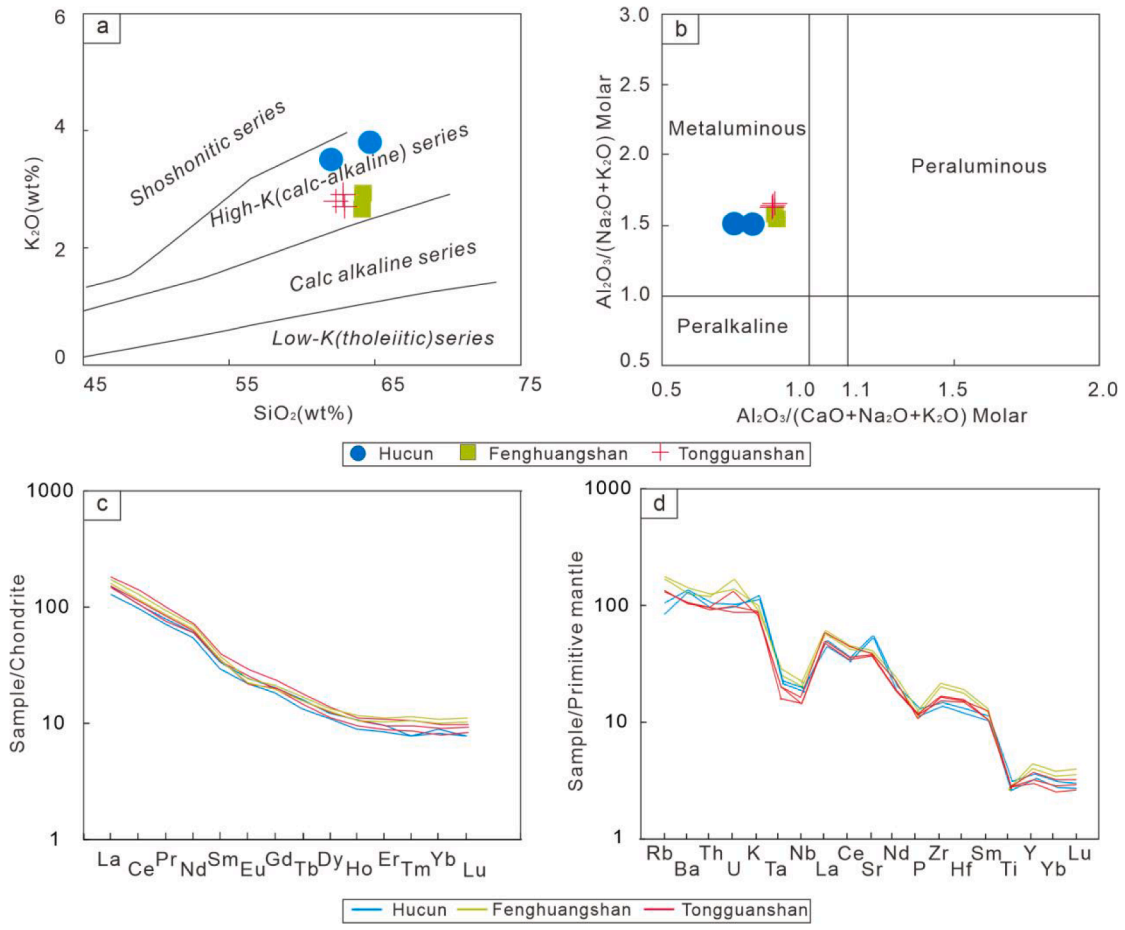

Fig. 4. K_2O vs SiO_2. The solid line is from Gill (1981) (a); the A/NK versus A/CNK diagram from Maniar and Piccoli (1989) (b), chondrite-normalized REE diagrams (c) and primitive mantle-normalized trace element diagrams (d) for the Hucun, Fenghuangshan, and Tongguanshan intrusions. The results are presented in Appendix 1. The chondrite and primitive mantle values are from Sun and McDonough (1989).

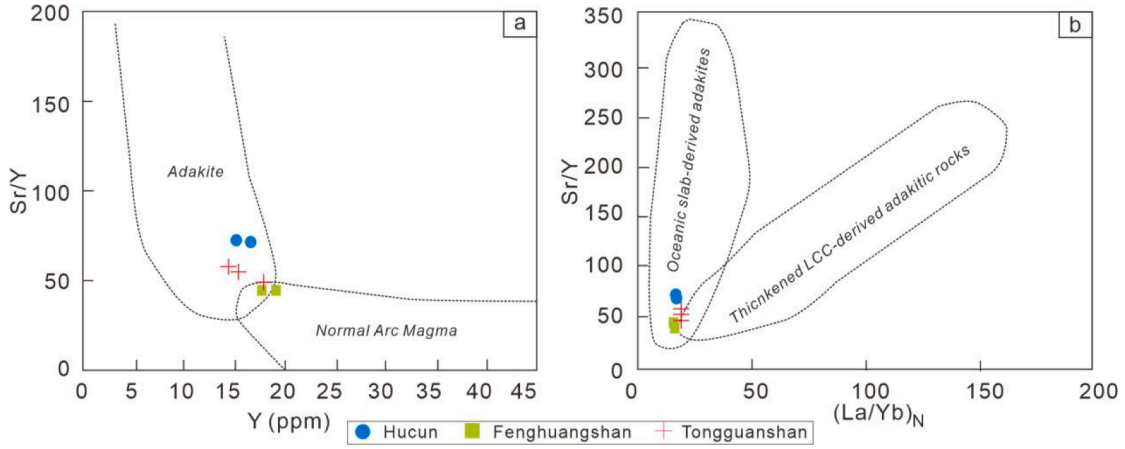

Fig. 5. Sr/Y versus Y classification diagram for identifying adakitic rocks (a) (Defant and Drummond, 1990); Sr/Y versus $(La/Yb)_N$ discriminant diagram to distinguish lower crust-derived adakitic rocks from slab-derived adakites (b) (Defant and Drummond, 1990; Liu et al., 2010).

4.4. Zircon trace elements

The zircon trace element contents are listed in Appendix 4. The high Th/U ratios (>0.1) suggest that the analyzed zircon crystals are igneous and have not been subjected to significant hydrothermal alteration (Moeller et al., 2003). The average Ce contents of zircon were 39.6 ppm, 20.8 ppm, and 31.4 ppm in the Tongguanshan, Fenghuangshan, and Hucun intrusions, respectively. The zircon Ce^{4+}/Ce^{3+} ratio was calculated using the method proposed by Ballard et al. (2002). The results revealed that the zircon Ce^{4+}/Ce^{3+} ratio was highest in the Hucun intrusion (265), moderate in the Tongguanshan intrusion (181), and lowest in the Fenghuangshan intrusion (159).

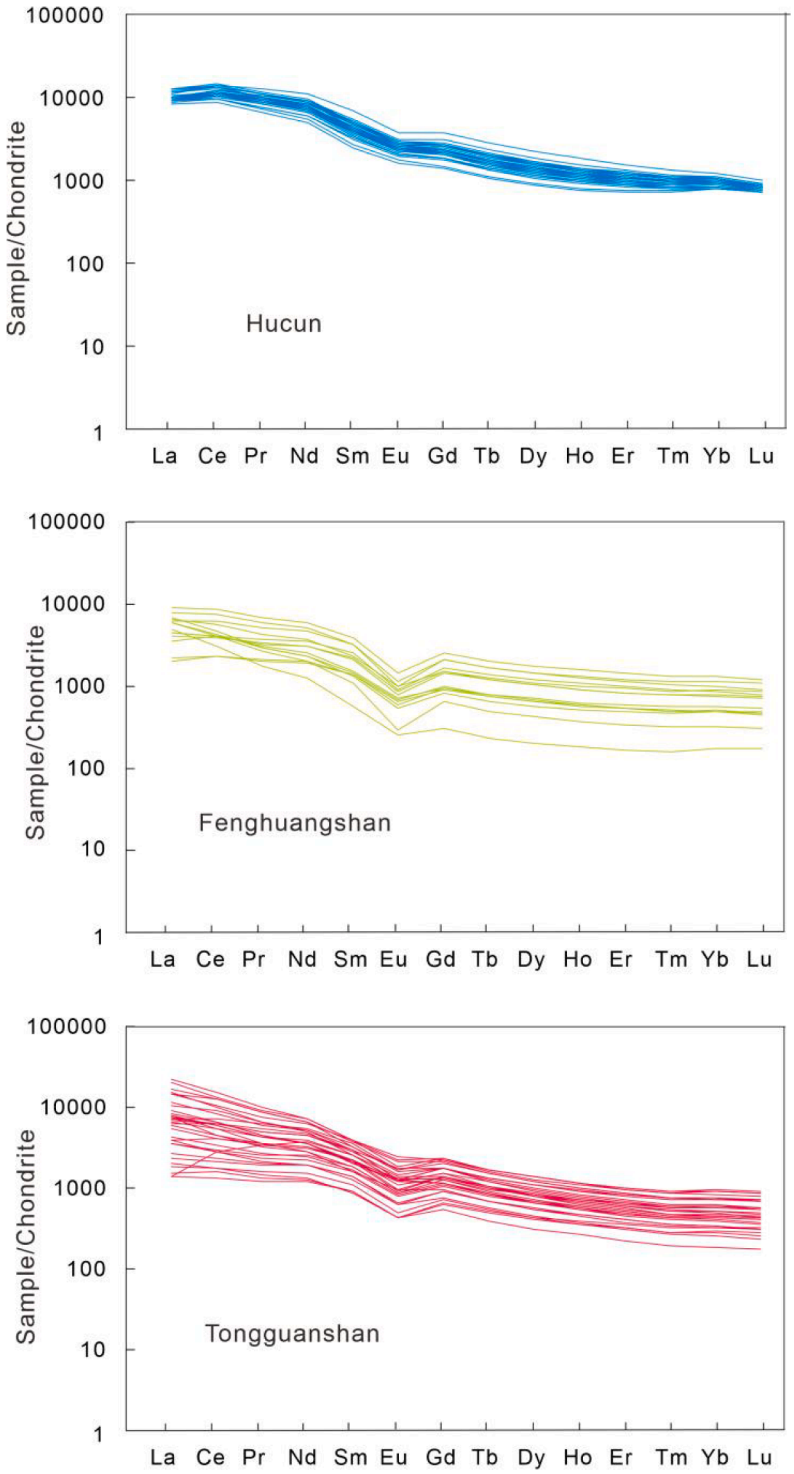

Fig. 6. Chondrite-normalized REE patterns for the titanite crystals from the selected intrusions. Data are listed in Appendix 2. The chondrite values are from Sun and McDonough (1989).

5. Discussions

5.1. Origin of analyzed titanite

The titanite grains in the three selected intrusions are igneous based on the textural observation. Titanites are identified to coexist with igneous plagioclase, amphibole, and quartz and are generally less altered, compared to the major minerals (Fig. 3 a–i). The euhedral and sub-euhedral morphologies (Fig. 3 a–i) indicate that titanite can crystallize before the magma evolved to its late stage. The BSE images show that titanite grains are less altered (Fig. 3 j–l). Although the alteration and recrystallization are visible in the edges and cracks of some titanite grains, the in situ microanalysis can avoid such areas and ensure the analyzed chemical composition is largely free from the interference of the post magmatic processes. This interpretation of the magmatic origin of the analyzed titanite is also supported by the titanite chemical composition. First, hydrothermal origin titanite tends to have flat chondrite-normalized REE patterns and depletion in light REEs

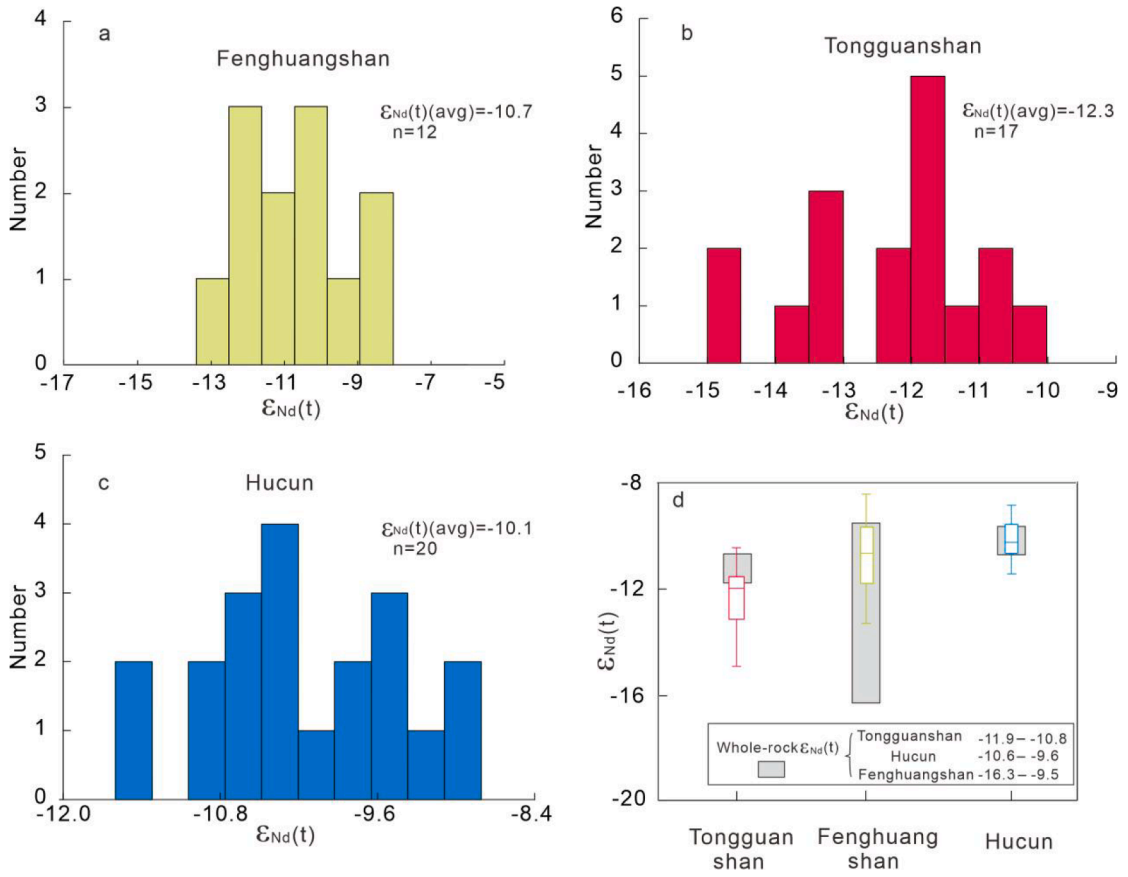

Fig. 7. Frequency histogram of titanite $\varepsilon_{Nd}(t)$ values of the Hucun, Fenghuangshan, and Tongguanshan intrusions. The whole-rock $\varepsilon_{Nd}(t)$ values are cited from Li et al. (2014) and Xu et al. (2019).

relative to heavy REEs (Aleinikoff et al., 2002; Chen et al., 2013; Papapavlou et al., 2017), neither of which was observed in our analyses. Second, the high REE (2418 ppm–21 040 ppm), Zr (55 ppm–2093 ppm), and Nb (117 ppm–2087 ppm) contents, negative Eu anomalies, and nearly flat heavy REE patterns of the analyzed titanites (Fig. 6) are consistent with those of igneous titanite (Xie et al., 2010; Gao et al., 2012; Jiang et al., 2016). Finally, it has also been suggested that hydrothermal origin titanite may be characterized by high U content (up to 2995 ppm) and low Th content (12.5 ppm–453 ppm) and low Th/U ratio (0.02–0.21) because the solubility of Th is relatively low compared to that of U in hydrothermal fluids (Hu et al., 2017). It follows that the titanites in this study which show relatively low U (42.89 ± 3.27 ppm–119.85 ± 129 ppm), high Th (174 ± 147 ppm–277 ± 47.9 ppm), and Th/U ratio (generally > 1) are not of hydrothermal origin.

5.2. Chemical composition variations of titanite

The ideal chemical formula of titanite is $CaTi(SiO_4)O$. The Ca sites of titanite can be occupied by Th, U, Mn, and REEs. Thorium U, and Mn showed good negative correlations with Ca in the Tongguanshan and Fenghuangshan titanites (Fig. 8 a–c), suggesting their direct replacement of Ca (Higgins and Ribbe, 1976; Deer et al., 1982). However, the above negative correlations are not reflected in the Hucun titanites. In view of the higher titanite REE content in the Hucun intrusion (15814 ± 1755 ppm) than that in other two intrusions (7118 ± 2784 ppm to 8588 ± 4814 ppm), the substitution of Ca in the Hucun titanite is mainly controlled by REE, whereas Th, U, and Mn may play a minor role in the substitution of Ca. Rare earth elements can replace Ca via the reaction $Ca^{2+}+Ti^{4+}=REE^{3+}+(Al^{3+}, Fe^{3+})$ (Franz and Spear, 1985; Bernau and Franz, 1987; Vuorinen and Halenius, 2005). The universality of this substitution is supported by the positive correlation between Ca and Ti (Fig. 8d) and the negative correlation between Ca and REEs in the analyzed titanites (Fig. 8e). The Ti sites of titanite can be occupied by Al, Fe, and Ga through the substitution reaction $Ca^{2+}+Ti^{4+}=REE^{3+}+(Al^{3+}, Fe^{3+}, Ga^{3+})$ (Franz and Spear, 1985; Bernau and Franz, 1987; Vuorinen and Halenius, 2005). The negative correlation between Ti and Al_2O_3, and FeO confirms that this substitution could have occurred in the analyzed titanite (Fig. 8f and g). However, the substitution of Ti by Ga was inconsequential because of the unclear positive correlation between Ti and Ga. Moreover, the indistinct negative correlation between Ti and Zr in the analyzed titanites (Fig. 8h) indicates that the direct substition of Ti^{4+} by Zr^{4+} (Cherniak, 2006) was not important or universal. In addition, Ti did not show any correlation with Nb + Ta (Fig. 8i), implying that the common substitution reaction $2Ti^{4+}=(Nb^{5+}, Ta^{5+})+(Al^{3+}, Fe^{3+})$ (Bernau and Franz, 1987; Cérny et al., 1995; Knoche et al., 1998; Cempírek et al., 2008; Lucassen et al., 2011) was negligible for the analyzed titanites. The O_1 titanite site can be occupied by F through the substitution reaction $Ti^{4+}+O^{2-}=(Al^{3+}, Fe^{3+})+F^{-}$ (Ribbe, 1980; Oberti et al., 1991; Enami et al., 1993; Markl and Piazolo, 1999; Troitzsch and Ellis, 2002), which led to a positive correlation between F and Al_2O_3 and FeO (Fig. 8j) in the titanites from the three intrusions.

5.3. Magmatic information related to Cu mineralization revealed by titanite

5.3.1. Magma oxidation state

The magma oxidation state has been recognized as crucial for porphyry-skarn Cu mineralization because high oxygen fugacity can prevent the early saturation of Cu-bearing sulfides, which ensures sufficient ore-forming element extraction via hydrothermal fluids from residual melt for later mineralization (Richards, 2015). Titanite typically contains a series of multivalent elements, such as Fe, Ga, Eu, and

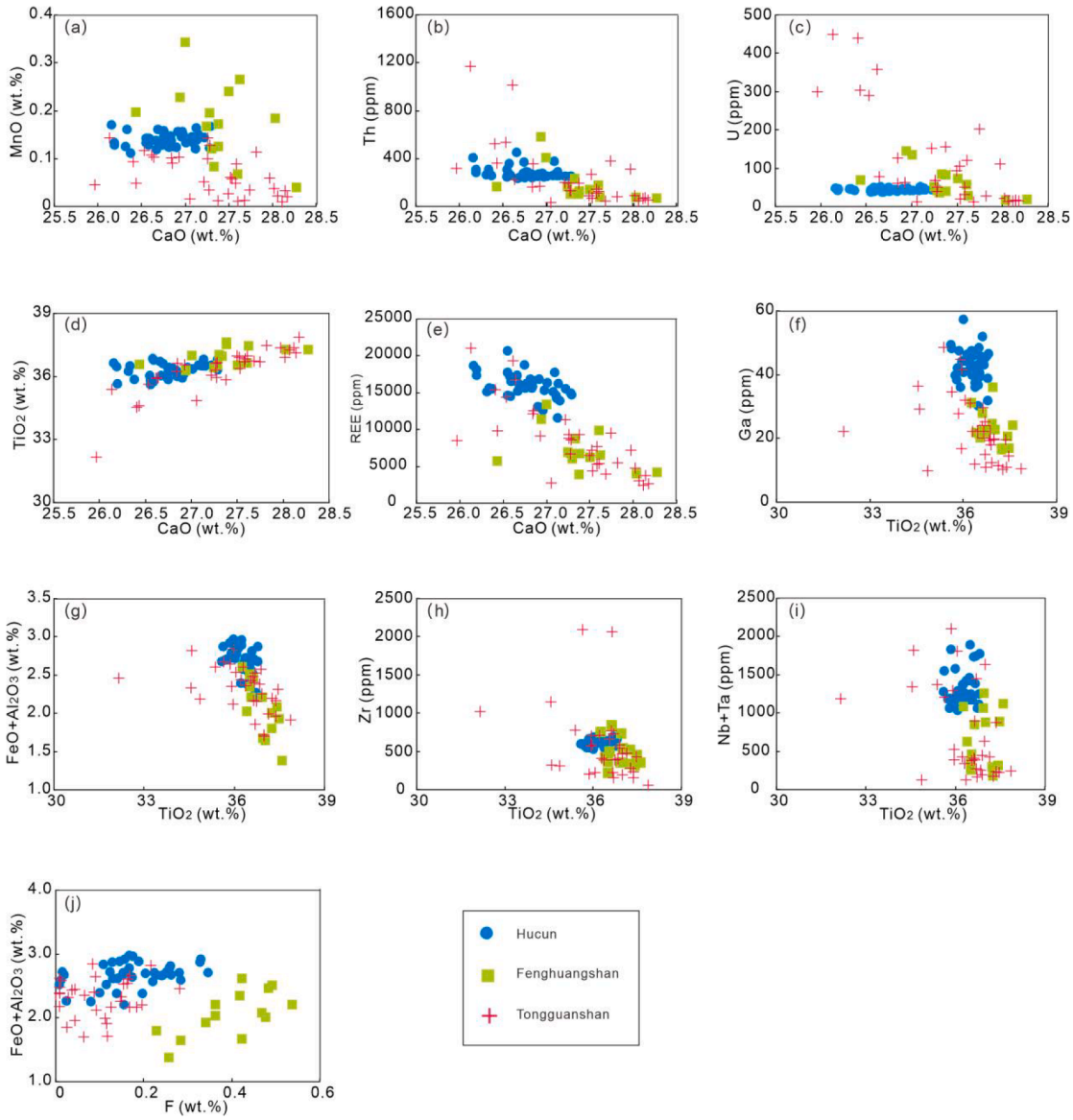

Fig. 8. Plots of CaO versus MnO (a); CaO versus Th (b); CaO versus U (c); CaO versus TiO_2 (d); CaO versus REE (e); TiO_2 versus Ga (f); TiO_2 versus FeO + Al_2O_3 (g); TiO_2 versus Zr (h); TiO_2 versus Nb + Ta (i); and F versus FeO + Al_2O_3 (j) in titanites from the selected intrusions.

Ce, which makes it useful for investigating the magma oxidation state. Studies have verified that compared to Ce^{4+} and Eu^{2+}, Ce^{3+} and Eu^{3+} have a better chance of occupying the Ca site of titanite because of their similar ionic radii to Ca^{2+}. Analogously, Fe^{3+} and Ga^{3+}, rather than Fe^{2+} and Ga^{2+}, are more likely to occupy the Ti sites of titanite (Tiepolo et al., 2002; King et al., 2013; Xu et al., 2015). Therefore, the increase in magmatic oxygen fugacity, which increases Ce^{4+}, Eu^{3+}, Fe^{3+}, and Ga^{3+} at the expense of Ce^{3+}, Eu^{2+}, Fe^{2+}, and Ga^{2+} in the melt, facilitates the incorporation of more Fe, Eu, and Ga by titanite, while suppressing the entry of Ce.

Our data show that whole-rock δEu values were almost consistent (0.83–1.01) among each of the selected intrusions, yet such values were more variable in titanites from these intrusions (0.35–0.87). Titanite δEu values can be influenced by the feldspar crystallization because feldspar is an important magmatic Eu sink (Bi et al., 2002; Xu et al., 2015). The existence of titanite in the interstitial gap of feldspar shown in Fig. 3a implies the possibility that some titanite grains may have crystallized simultaneously or later than feldspar grains. Therefore, it is necessary to evaluate the influence of feldspar crystallization on the titanite δEu value. In fact, as feldspar is enriched in Sr, if feldspar crystallization results in a large reduction in the titanite δEu value, then a decrease in the Sr content in titanite should also occur; however, a positive correlation between Sr and δEu was not observed in the analyzed titanites (Fig. 9a). We observed that the Fenghuangshan intrusion has lower titanite δEu value than that for the Tongguanshan intrusion. If this is caused by more feldspar crystallization in the magma system of the former intrusion than the latter, correspondingly, lower titanite Sr content would emerge in the Fenghuangshan intrusion. However, the hypothesis contradicts the fact that the titanites from the Fenghuangshan intrusion contain much more Sr than those from the Tongguanshan intrusion. The decoupling of titanite Sr content and δEu value further suggests that although the influence of feldspar on titanite δEu value cannot be entirely ruled out, at least it is insignificant for the titanites investigated. This conjecture is reasonable, because porphyry Cu mineralization usually requires rich H_2O in magma that can lead to the suppression of feldspar crystallization (Richards and Kerrich, 2007). The existence of amphibole grains in all three intrusions is convincing evidence of rich H_2O in the magma because previous studies have confirmed that the H_2O content of magmas saturated with amphibole usually exceeds 4 wt% (Naney, 1983; Ridolfi et al., 2010; Loucks 2014).

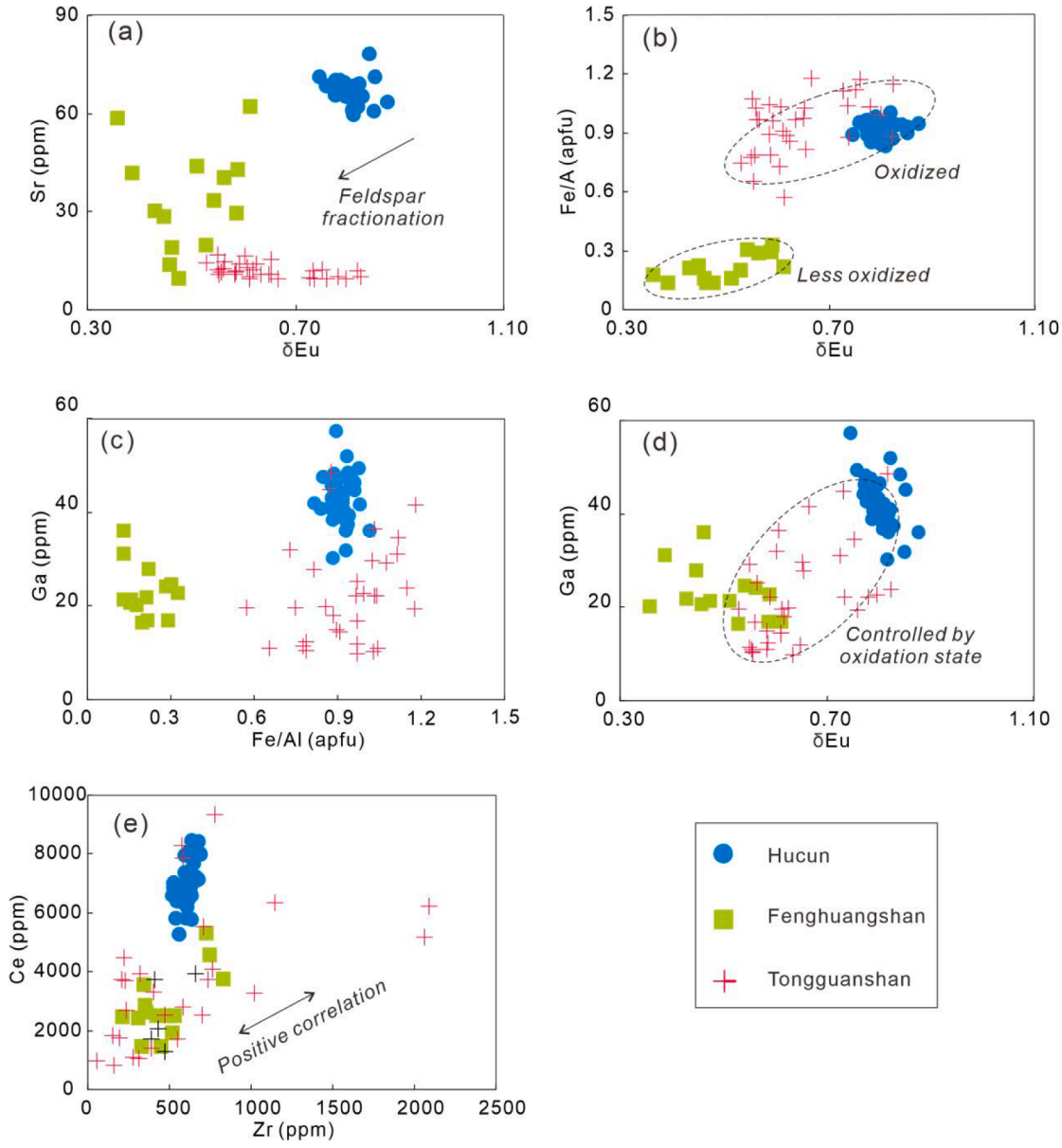

Fig. 9. Plots of δEu versus Sr (a); δEu versus Fe/Al (b); Fe/Al versus Ga (c); δEu versus Ga (d); and Zr versus Ce (e) in titanites from the selected intrusions.

It can be inferred that only a small amount of feldspar crystallized earlier than or simultaneously with the titanite, which failed to bring about significant chemical influence on the titanite. After excluding the significant interference of feldspar crystallization, the change of the titanite δEu value is considered to be predominantly controlled by magma oxidation state. The lower titanite δEu values (approximately 0.5) in the Fenghuangshan intrusion probably indicate a less-oxidized magma system of this intrusion compared to that of the Hucun and Tongguanshan intrusions (0.64–0.80).

The same conclusion was reached for the titanite Fe/Al ratio (atoms per formula unit). As mentioned above, the increase in Fe^{3+} in the melt, owing to the increase in oxygen fugacity, would facilitate the incorporation of more Fe into titanite to substitute Ti, and an elevated Fe/Al ratio can be formed. Our data shows that the Fenghuangshan intrusion had a moderate whole-rock Fe/Al ratio among the three intrusions; however, the titanites from this intrusion have much lower Fe/Al ratios (0.13–0.32) than those from the other two intrusions (0.57–1.17). This decoupling of the Fe/Al value characteristics between the titanites and their host rocks indicates that the titanite Fe/Al ratio is not a reflection of the magmatic Fe/Al ratio. Moreover, the Fe/Al ratio of titanite may be influenced by the pressure conditions during the formation of titanite (Hellman and Green, 1979; Franz and Spear, 1985); however, the calculated pressures based on a method of Zr-in-titanite proposed by Hayden et al. (2008) were similar among the three intrusions (Hucun: 2.15 GPa, Fenghuangsahn: 2.27 GPa, and Tongguanshan: 2.11 GPa). Therefore, we speculate that the difference in titanite Fe/Al ratios is more likely a result of differing magma oxidation states among the three intrusions. The lower Fe/Al ratio and δEu values in the Fenghuangshan titanite demonstrate that the causative magma of this intrusion is indeed less oxidized than those of the other studied intrusions (Fig. 9b).

The Ga content and δCe value in titanite may be affected by the magma oxidation state (King et al., 2013; Xu et al., 2015). Notably, if the Ga content of titanite is primarily determined by the magma oxidation state, then the increase in oxygen fugacity will lead to synchronously elevated Ga content, Fe/Al ratios, and δEu values in titanite; however, such a positive correlation among these oxygen fugacity proxies is not present in the Hucun or Fenghuangshan titanites (Fig. 9 c–d). The premise that the titanite δCe value indicates the magma oxidation state is founded on the speculation that Ce enters titanite mainly in the form of Ce^{3+}, rather than Ce^{4+}; however, a recent study showed that Ce^{4+} can

also be incorporated into titanite through the following reaction: $Ce^{4+}+Zr^{4+}=Eu^{3+}+(Nb^{5+}, Ta^{5+})$ (King et al., 2013). The positive correlation between Ce and Zr (Fig. 9e) further suggests that this substitution prevailed in the studied titanite. As a result, these two proxies are not applicable for investigating the magma oxidation states of the three intrusions.

Finally, to independently verify the magma oxidation state identified by titanite, we calculated the zircon Ce^{4+}/Ce^{3+} values of each intrusion. Our results show that the zircon Ce^{4+}/Ce^{3+} value was highest in the Hucun intrusion (265), moderate in the Tongguanshan intrusion (181), and lowest in the Fenghuangshan intrusion (159). The magma oxidation state revealed by the zircon Ce^{4+}/Ce^{3+} values was consistent with the titanite results. Although the parental magma of the Fenghuangshan intrusion is less oxidized than those of the other two intrusions, the high zircon Ce^{4+}/Ce^{3+} values of this intrusion (>120–50, Liang et al., 2006; Wang et al., 2014; Shen et al., 2015) indicate that it was oxidized enough to form important porphyry Cu mineralization. Our results further show that titanites crystallizing from the oxidized magma system have elevated δEu values (>0.5) and Fe/Al ratios (>0.2), and that there was a slight positive correlation between these two proxies. We speculate that these titanite proxies may potentially be used to evaluate whether magma oxidation states are suitable for porphyry-skarn Cu mineralization and are effective for at least the three intrusions.

5.3.2. Magmatic F abundance

During the upwelling of ore-forming magma, hydrothermal fluid is eventually exsolved owing to the decreasing pressure. Hydrothermal fluid exsolution can extract H_2O and Cl from the melt, but can hardly consume F unless in a very late stage of magma evolution; this is thought to be the case because experimental results have shown that F tends to be enriched in residual melt rather than hydrothermal fluid (Candela, 1986; Warner et al., 1998). Therefore, a scenario is expected that if titanite can crystallize early, and there is no extensive crystallization of F-bearing minerals during titanite crystallization, titanite F contents may be indicative of the abundance of F in the melt. The analysis results of this study show that the F content of titanite in the Fenghuangshan intrusion is nearly-two times higher than that of titanite from the other two intrusions. We deduce that this is a response to a higher magmatic F abundance in the Fenghuangshan intrusion than that in the other two intrusions for the following reasons. First, the euhedral and subeuhedral morphologies indicate that titanites from these intrusions can crystallize relatively early from magma. Second, there are few F-rich minerals (no fluorite, and only sparse apatite) in the rock samples. The amphibole and biotite as the important carriers of Fe and Al in intermediate-acid magmas, also contain a small amount of F. If the lower F content of titanite in the Tongguanshan and Hucun intrusions than that in the Fenghuangshan intrusion was caused by the crystallization of amphibole and biotite, correspondingly, the Fe + Al content of titanite in the first two intrusions should also be lower than that in the latter intrusion. This, however, is in contradiction with the fact that the Tongguanshan and Hucun intrusions have a higher Fe + Al content of titanite than the Fenghuangshan intrusion.

It has been recognized that F enrichment in magma can facilitate the hydrothermal mineralization of some trace elements such as Nb, Ta, and REEs because the increased F can enhance the solubility of these elements and prolong the duration of magmatic differentiation by depolymerizing the melt (Huang et al., 2018; Wu et al., 2020). With magmatic differentiation, these elements would continuously concentrate in the residual melt, greatly improving the extraction efficiency of ore-forming elements via hydrothermal fluid; however, F has been proven to have a negligible effect on the Cu solubility in the melt and is not involved in Cu partitioning between the melt and hydrothermal fluid (Keppler and Wyllie, 1991). Therefore, F may not play an important role in porphyry-skarn Cu mineralization. Furthermore, we compared the titanite F content of the studied intrusions with that of several non-Cu-mineralized intrusions in the Nanling region of southern China (Wang et al., 2011). Our results showed that the titanites from the three Cu-mineralized intrusions do not contain more F than those from the intrusions without Cu mineralization (Fig. 10). The differences in titanite F content between intrusions with different Cu-mineralized potential may imply that the requirement for high magmatic F enrichment for Cu mineralization related to magmatic hydrothermal fluid is not universal.

5.3.3. Implications for petrogenetic model of Cu-mineralized intrusions

As a result of recent technological advances, the precise detection of the in situ Nd isotope composition of titanite has become feasible (Xie et al., 2010; Cao et al., 2015). In this study, the Nd isotope data show that titanites from all three intrusions have approximate $\varepsilon_{Nd}(t)$ values (Tongguanshan titanite: −14.9 to -10.4, Fenghaungshan titanite: −13.5 to -8.5, and Hucun titanite: −11.4 to -8.8) to their host rocks (Tongguanhan intrusion: −11.9 to -10.8, Fenghuangshan intrusion: −16.3 to -9.5, and Hucun intrusion: −10.6 to -9.6) (Li et al., 2014; Xu et al., 2019) (Fig. 7). The results confirm that titanite can effectively inherit the Nd isotopic composition of host rocks. Because rock samples may not preserve the initial isotopic Nd characteristics owing to serious alteration and weathering (Liu et al., 2015), the titanite Nd isotope is becoming a new way to track the initial Nd isotope composition of altered rocks.

The Nd isotope characteristics of titanite in this study could provide an implication for the petrogenesis of the investigated Cu-mineralized intrusions. There are several petrogenetic models for the Cu-mineralized intrusions in the Tongling ore district, including partial melting of the Yangtze lower crust (Zhang et al., 2001), the mixing between mantle-derived basic magma and crust-derived magma (Chen and Jahn, 1998; Chen et al., 2016), and partial melting of the subducted oceanic crust (Ling et al., 2009; Liu et al., 2010; Li et al., 2014; Xie et al., 2018; Jiang et al., 2020). Given that the $\varepsilon_{Nd}(t)$ value of the Yangtze lower crust represented by the Archean Kongling Group is less than −25 (Guo et al.,2014), the higher $\varepsilon_{Nd}(t)$ values in the titanites and their host rocks indicate that the Yangtze lower crust is not a suitable magma source of the Cu-mineralized intrusions. Therefore, the first model can be excluded to some extent. The other two models could explain the "juvenile" Nd isotopic characteristics in titanite and its host rocks relative to that in the ancient lower continental crust. However, based on the similarity of whole-rock geochemical signatures such as Sr/Y and $(La/Yb)_N$ between three intrusions investigated and the ocean slab-derived adakites (Fig. 5b), we prefer the third model. A recent study depicted more details of this model including the mixing of slab melt with marine sediments, and magmatic contamination by enriched mantle-derived and ancient crustal-derived materials during magma ascent and emplacement (Wang et al., 2022). Considering that ocean slab subduction may bring abundant H_2O, CO_2, and Fe^{3+} into the mantle wedge and cause it to be oxidized (Mungall, 2002; Kelley and Cottrell, 2009), the oxygen fugacity of slab-derived melt would be elevated owing to its possible contamination by metasomatized overlying mantle wedge during its ascent. The petrogenetic model explains the possible origin of high magmatic oxygen fugacity in the Cu-mineralized intrusions such as Hucun, Fenghuangshan and Tongguanshan.

It is notable that some Cretaceous adakitic intrusions in the Dabie orogenic belt close to the Tongling ore district have a weak ability for porphyry-skarn Cu mineralization (Liu et al., 2010; Sun et al., 2010). The Cu-barren adakitic intrusions exhibit more negative whole-rock $\varepsilon_{Nd}(t)$ values (mostly < −15, even <−20) than the Cu-mineralized intrusions in the Tongling ore district (Huang et al., 2008; Liu et al., 2010), which was explained as the magma originating from the partial melting of delaminated lower continental crust instead of oceanic crust (Huang et al., 2008; Liu et al., 2010). This view provides us with an understanding that the difference in magma source may be an important controlling factor of the Cu mineralization potential of adakites in the Dabie-Tongling area. Admittedly, it is insufficient to reveal magma sources only through titanite Nd isotopes, in consideration of the different Nd isotope compositions in magma systems with different Cu mineralized potential, titanite Nd isotopes may be an auxiliary

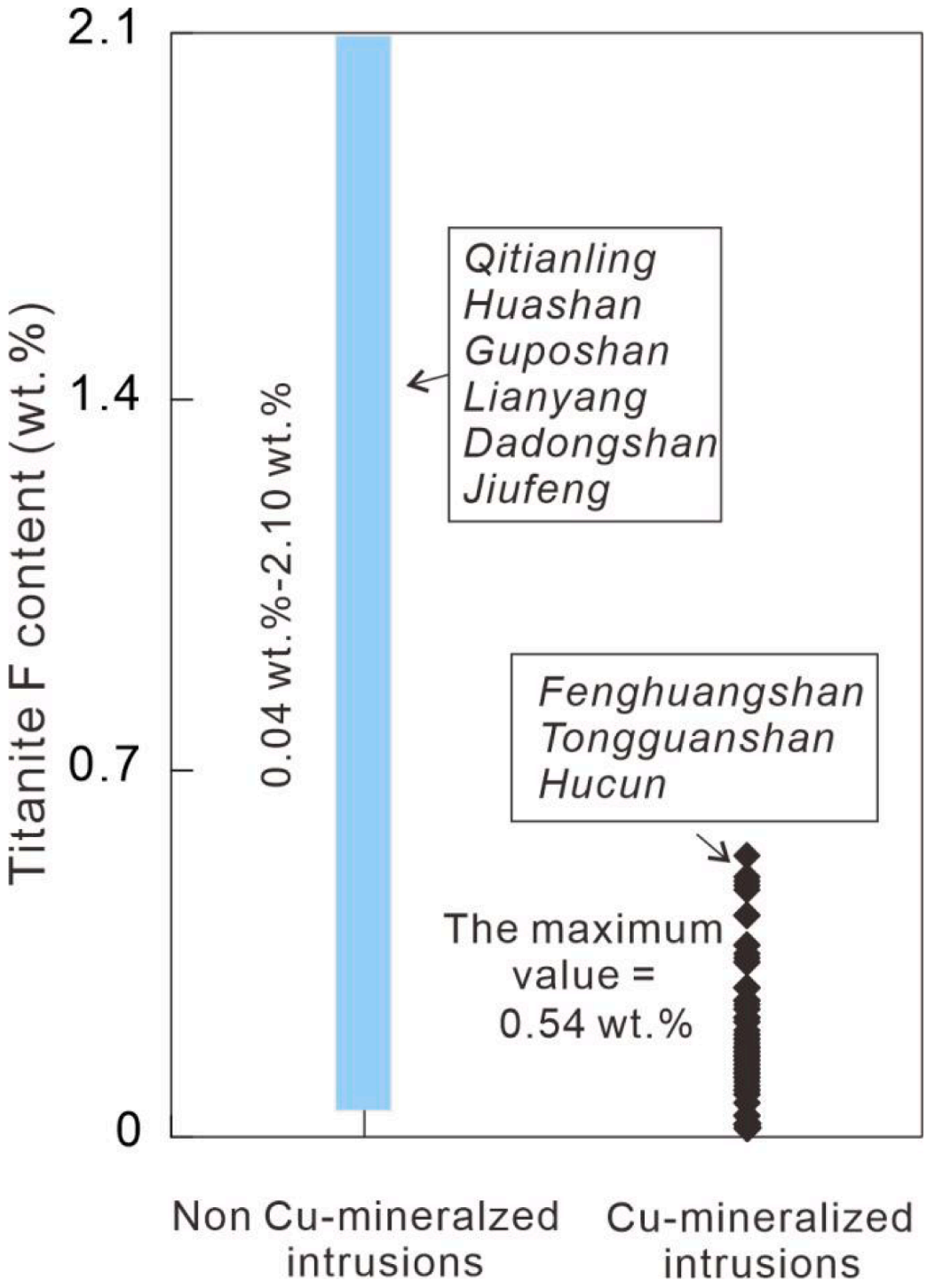

Fig. 10. Comparison of titanite F content between the Cu-mineralized and non-Cu-mineralized intrusions. The data of the non-Cu-mineralized intrusions are cited from Wang et al. (2011).

prospecting indicator of adakitic rocks, especially when the rock samples cannot preserve the initial Nd isotope composition due to alteration and weathering.

6. Conclusions

Three Cu-mineralized intrusions (Hucun, Tongguanshan, and Fenghaungshan) in the Tongling ore district of eastern China were selected to investigate the applicability of geochemical titanite proxies in indicating the physical and chemical nature of magma systems related to magmatic hydrothermal Cu mineralization. The textural observation and chemical composition of titanite indicate that the analyzed titanites were of magmatic origin and can thus be used to trace magmatic information. Specifically, the titanite δEu values and Fe/Al ratios are useful indicators of the magma oxidation state, and the titanite F content and Nd isotopes reflect the magmatic composition. The titanite geochemistry demonstrates that the causative magma of the Fenghuangshan intrusion is less oxidized and contains more F than that of the Tongguanshan and Hucun intrusions. Our results suggest that magma with high oxygen fugacity may have a relatively high potential

for porphyry-skarn Cu mineralization; however, the enrichment of F in magma is not necessary for this mineralization. In addition, our results indicate that titanite Nd isotope can effectively inherit the Nd isotope characteristics of magma and may be an auxiliary indicator for ore prospecting of adakites. Our findings confirm that titanite has great potential for indicating the magmatic physical and chemical nature of the dioritic intrusions associated with porphyry-skarn Cu deposits.

Declaration of Competing Interest

The authors declare that they have no known competing financial interests or personal relationships that could have appeared to influence the work reported in this paper.

Data availability

No data was used for the research described in the article.

Acknowledgments

This study was supported by the National Natural Science Foundation of China (Grant 42173069), Guizhou Provincial Science and Technology Projects (QKHJC-ZK[2021] YB211), "Light of West China" Program of Chinese Academy of Sciences, and Frontier project of State Key Laboratory of deposit geochemistry, Institute of geochemistry, Chinese Academy of Sciences. We thank Yan-Wen Tang and Zhi-Hui Dai for their assistance in titanite and zircon trace element analysis by LA-ICP-MS, Wen-Qin Zheng and Xiang Li for their support in titanite chemical analysis by EPMA, You-Wei Chen for his help in titanite Nd isotope analysis by LA-MC-ICP-MS and Shu-Qin Yang and Jing Hu for their assistance in the whole-rock chemical analysis by XRF and ICP-MS. Two anonymous reviewers are greatly thanked for their constructive comments and suggestions which has greatly improved the manuscript.

Appendix A. Supplementary data

Supplementary data to this article can be found online at https://doi.org/10.1016/j.oregeorev.2022.105219.

References

Aleinikoff, J.N., Wintsch, R.P., Fanning, C.M., Dorais, M.J., 2002. U-Pb geochronology of zircon and polygenetic titanite from the Glastonbury Complex, Connecticut, USA: an integrated SEM, EMPA, TIMS, and SHRIMP study. Chem. Geol. 188, 125–147.
Aleksandrov, S.M., Troneva, M.A., 2007. Composition, mineral assemblages, and genesis of titanite and malayaite in skarns. Geochem. Int. 45, 1012–1024.
Bachmann, O., Dungan, M.A., Bussy, F., 2005. Insights into shallow magmatic processes in large silicic magma bodies: the trace element record in the Fish Canyon magma body, Colorado. Contrib. Mineral. Petr. 43, 1469–1503.
Bernau, V.R., Franz, G., 1987. Crystal chemistry and genesis of Nb-, V-and Al-rich metamorphic titanite from Egypt and Greece. Can. Mineral. 25, 695–705.
Bi, X.W., Cornell, D.H., Hu, R.Z., 2002. REE composition of primary and altered feldspar from the mineralized alteration zone of alkali-rich intrusive rocks, Western Yunnan Province, China. Ore Geol. Rev. 19, 69–78.
Buick, I.S., Hermann, J., Mass, R., Gibson, R.L., 2007. The timing of subsolidus hydrothermal alteration in the Central Zone, Limpopo Belt (South Africa): constraints from titanite U-Pb geochronology and REE partitioning. Lithos 98, 97–117.
Candela, P.A., 1986. Toward a thermodynamic model for the halogens in magmatic systems: an application to melt-vapor-apatite equilibria. Chem. Geol. 57, 289–301.
Cao, M.J., Qin, K.Z., Li, G.M., Evans, N.J., Jin, L.Y., 2015. In situ LA-(MC)-ICP-MS trace element and Nd isotopic compositions and genesis of polygenetic titanite from the Baogutu reduced porphyry Cu deposit, Western Junggar, NW China. Ore Geol. Rev. 65, 940–954.
Cao, M.J., Evans, N.J., Hollings, P., Cooke, D.R., McInnes, B.I.A., Qin, K.Z., Li, G.M., 2018. Phenocryst zonation in porphyry-related rocks of the Baguio District, Philippines: Evidence for magmatic and metallogenic processes. J. Petrol. 59, 825–848.
Cao, Y., Zheng, Z.J., Du, Y.L., Gao, F.P., Qin, X.L., Yang, H.M., Lu, Y.H., Du, Y.S., 2017. Ore geology and fluid inclusions of the Hucunnan deposit, Tongling, Eastern China: Implications for the separation of copper and molybdenum in skarn deposits. Ore Geol. Rev. 83, 152–173.
Cempírek, J., Houzar, S., Novák, M., 2008. Complexly zoned niobian titanite from hedenbergite skarn at Písek, Czech Republic, constrained by substitutions Al(Nb, Ta)T_i-2, Al(F, OH)(Ti_O)-1 and Sn_Ti-1. Mineral. Mag. 72, 1293–1305.
Cérny, P., Novák, M., Chapman, R., 1995. The Al(Nb, Ta)Ti(in-2) substitution in titanite: the emergence of a new species? Miner. Petrol. 52, 61–73.
Chang, Y.F., Liu, X.P., Wu, Y.C., 1991. The Copper–iron Belt of the Middle and Lower Reaches of the Changjiang River. Geological Publishing House, Beijing, p. 379 in Chinese with English abstract.
Che, X.D., Linnen, R.L., Wang, R.C., Groat, L.A., Brand, A.A., 2013. Distribution of trace and rare earth elements in titanite from tungsten and molybdenum deposits in Yukon and British Columbia, Canada. Can. Mineral. 51, 415–438.
Chen, C.J., Chen, B., Li, Z., Wang, Z.Q., 2016. Important role of magma mixing in generating the Mesozoic monzodioritic-granodioritic intrusions related to Cu mineralization, Tongling, East China: Evidence from petrological and in situ Sr–Hf isotopic data. Lithos 248–251, 80–93.
Chen, J., Jahn, B.M., 1998. Crustal evolution of southeastern China: Nd and Sr isotopic evidence. Tectonophysics 284, 101–133.
Chen, Y.X., Zheng, Y.F., Hu, Z.C., 2013. Polyphase growth of accessory minerals during continental collision: geochemical evidence from ultrahigh-preesure metamophic gneisses in the Sulu orogen. Lithos 177, 245–267.
Cherniak, D.J., 2006. Zr diffusion in titanite. Contrib. Mineral. Petr. 152, 639–647.
Deer, W.A., Howie, R.A., Zussman, J., 1982. Rock forming minerals. Orthosilicates, 1A. Longman, London.
Defant, M.J., Drummond, M.S., 1990. Derivation of some modern arc magmas by melting of young subducted lithosphere. Nature 347, 662–665.
Deng, J., Wang, Q.F., Xiao, C.H., Yang, L.Q., Liu, H., Gong, Q.J., Zhang, J., 2011. Tectonic-magmatic-metallogenic system, Tongling ore cluster region, Anhui Province. China. Int. Geol. Rev. 53, 449–476.
Enami, M., Suzuki, K., Liou, J.G., Bird, D.K., 1993. Al-Fe^{3+} and F-OH substitutions in titanite and constraints on their P-T dependence. Eur. J. Mineral. 5, 219–231.
Faure, M., Sun, Y., Shu, L., Monié, P., Charvet, J., 1996. Extensional tectonics within a subduction-type orogen. The case study of the Wugongshan dome (Jiangxi Province, southeastern China). Tectonophysics 263, 77–106.
Franz, G., Spear, F.S., 1985. Aluminous titanite (sphene) from the eclogite zone, south-central Tauern Window, Austria. Chem. Geol. 50, 33–46.
Gao, X.Y., Zheng, Y.F., Chen, Y.X., Guo, J.L., 2012. Geochemical and U-Pb age constraints on the occurrence of polygenetic titanite in UHP metagranite in the Dabie orogen. Lithos 136–139, 93–108.
Gill, J.B., 1981. Orogeneic Andesites and Plate Tectonics. Springer-Verlag, Berlin, p. 390.
Glazner, A.F., Coleman, D.S., Bartley, J.M., 2008. The tenuous connection between high-silica rhyolites and granodiorite plutons. Geology 36, 183–186.
Guo, J.L., Gao, S., Wu, Y.B., Li, M., Chen, K., Hu, Z.C., Liang, Z.W., Liu, Y.S., Zhou, L., Zong, K.Q., Zhang, W., Chen, H.H., 2014. 3.45 Ga granitic gneisses from the Yangtze Craton, South China: Implications for Early Archean crustal growth. Precambr. Res. 242, 82–95.
Hayden, L., Watson, E.B., Wark, D.A., 2008. A thermobarometer for sphene (titanite). Contrib. Mineral. Petr. 155, 529–540.
Hellman, P.L., Green, T.H., 1979. The role of sphene as an accessory phase in the high-pressure partial melting of hydrous mafic compositions. Earth Planet. Sc. Lett. 42, 191–201.
Higgins, J.B., Ribbe, P.H., 1976. The crystal chemistry and space groups of natural and synthetic titanites. Am. Mineral. 61, 878–888.
Hu, H., Li, J.W., McFarlane, C.R.M., 2017. Hydrothermal titanite from the Chengchao iron skarn deposit: temporal constraints on iron mineralization, and its potential as a reference material for titanite U-Pb dating. Mineral. Petrol. 111, 593–608.
Huang, F., Li, S.G., Dong, F., He, Y.S., Chen, F.K., 2008. High-Mg adakitic rocks in the Dabie orogen, central China: Implications for foundering mechanism of lower continental crust. Chem. Geol. 255, 1–13.
Huang, H., Wang, T., Zhang, Z.C., 2018. Highly differentiated fluorine-rich, alkaline granitic magma linked to rare metal mineralization: A case study from the Boziguo'er rare metal granitic pluton in South Tianshan Terrane, Xinjiang, NW China. Ore Geol. Rev. 96, 146–163.
Isnard, H., Brennetot, R., Caussignac, C., Caussignac, N., Chartier, F., 2005. Investigations for determination of Gd and Sm isotopic compositions in spent nuclear fuels samples by MC ICPMS. Int. J. Mass Spectrom. 246, 66–73.
Jiang, X.Y., Deng, J.H., Luo, J.C., Zhang, L.P., Luo, Z.B., Yan, H.B., Sun, W.D., 2020. Petrogenesis of Early Cretaceous adakites in Tongguanshan Cu-Au polymetallic deposit, Tongling region, eastern China. Ore Geol. Rev. 126, 103717.
Jiang, P., Yang, K.F., Fan, H.R., Liu, X., Cai, Y.C., Yang, Y.H., 2016. Titanite-scale insight into multi-stage magma mixing in Early Cretaceous of NW Jiaodong terrane, North China Craton. Lithos 258–259, 197–214.
Keppler, H., Wyllie, P.J., 1991. Partitioning of Cu, Sn, Mo, W, U, and Th between melt and aqueous fluid in the systems haplogranite-H_2O-HCl and haplogranite-H_2O-HF. Contrib. Mineral. Petr. 109, 139–150.
King, P.L., Sham, T.K., Gordon, R.A., Dyar, M.D., 2013. Microbeam X-ray analysis of Ce^{3+}/Ce^{4+} in Ti-rich minerals: A case study with titanite (sphene) with implications for multivalent trace element substitution in minerals. Am. Mineral. 98, 110–119.
Knoche, R., Angel, R.J., Seifert, F., Fliervoet, T.F., 1998. Complete substitution of Si for Ti in titanite $Ca(Ti_{1-x}Si_x)^{VI}Si^{IV}O_5$. Am. Mineral. 83, 1168–1175.
Li, Z.X., Li, X.H., 2007. Formation of the 1300-km-wide intracontinental orogen and postorogenic magmatic province in Mesozoic South China: A flat-slab subduction model. Geology 35, 179–182.
Li, S., Yang, X.Y., Huang, Y., Sun, W.D., 2014. Petrogenesis and mineralization of the Fenghuangshan skarn Cu–Au deposit, Tongling ore cluster field, Lower Yangtze metallogenic belt. Ore Geol. Rev. 58, 148–162.

Liang, H.Y., Campbell, I.H., Allen, C., Sun, W.D., Liu, C.Q., Yu, H.X., Xie, Y.E., Zhang, Y. Q., 2006. Zircon Ce^{4+}/Ce^{3+} ratios and ages for Yulong ore-bearing porphyries in eastern Tibet. Miner. Deposita 41, 152–159.
Ling, M.-X., Wang, F.-Y., Ding, X., Hu, Y.-H., Zhou, J.-B., Zartman, R.E., Yang, X.-Y., Sun, W., 2009. Cretaceous ridge subduction along the Lower Yangtze River belt, eastern China. Econ. Geol. 104 (2), 303–321.
Liu, Y.S., Hu, Z.C., Gao, S., Gunther, D., Xu, J., Gao, C.G., Chen, H.H., 2008. In situ analysis of major and trace elements of anhydrous minerals by LA-ICP-MS without applying an internal standard. Chem. Geol. 257, 34–43.
Liu, S.A., Li, S.G., He, Y.S., Huang, F., 2010. Geochemical contrasts between early Cretaceous ore-bearing and ore-barren high-Mg adakites in central–eastern China: implications for petrogenesis and Cu–Au mineralization. Geochim. Cosmochim. Ac. 74, 7160–7178.
Liu, L.M., Peng, S.L., 2004. Prediction of hidden ore bodies by synthesis of geological, geophysical and geochemical information based on dynamic model in Fenghuangshan ore field, Tongling district, China. J. Geochem. Explor. 81, 81–98.
Liu, Z.F., Shao, Y.J., Wang, C., Liu, Q.Q., 2019. Genesis of the Dongguashan skarn Cu-(Au) deposit in Tongling, Eastern China: Evidence from fluid inclusions and H-O-S-Pb isotopes. Ore Geol. Rev. 104, 462–476.
Liu, Y.H., Yang, H.J., Takazawa, E., Satish-Kumar, M., You, C.F., 2015. Decoupling of the Lu-Hf, Sm-Nd, and Rb-Sr isotope systems in eclogites and a garnetite from the Sulu ultra-high pressure metamorphic terrane: causes and implications. Lithos 234–235, 1–14.
Loucks, R.R., 2014. Distinctive composition of copper-ore-forming arcmagmas. Aust. J. Earth Sci. 61, 5–16.
Lowell, D.E., Guilbert, J.M., 1970. Lateral and vertical alteration-mineralization zoning in porphyry ore deposits. Econ. Geol. 65, 373–408.
Lu, S.M., Xu, X.C., Xie, Q.Q., Lou, J.W., Chu, G.Z., Xiong, Y.P., 2007. Chemical and stable isotope geochemical characteristics of ore-forming fluid of the Shizishan copper and gold ore-field, Tongling, China. Acta Petrol. Sin. 23, 177–184.
Lucassen, F., Franz, G., Dulski, P., Romer, R.L., Rhede, D., 2011. Element and Sr isotope signature of titanite as indicator of variable fluid composition in hydrated eclogite. Lithos 121, 12–24.
Maniar, P.D., Piccoli, P.M., 1989. Tectonic discrimination of granitoids. Geol. Soc. Am. Bull. 101, 635.
Mao, J.W., Wang, Y.T., Lehmann, B., Du, A.D., Mei, Y.X., Li, Y.F., Zang, W.S., Stein, H.J., Zhou, T.F., 2006. Molybdenite Re-Os and albite 40Ar/39Ar dating of Cu-Au-Mo and magnetite porphyry systems in the Yangtze River valley and metallogenic implications. Ore Geol. Rev. 29, 307–324.
Mao, J.W., Xie, G.Q., Duan, C., Pirajno, F., Ishiyama, D., Chen, Y.C., 2011. A tectono-genetic model for porphyry-skarn-stratabound C-Au-Mo-Fe and magnetite-apatite deposits along the Middle-Lower Yangtze River Valley. Eastern China. Ore Geol. Rev. 43, 294–314.
Markl, G., Piazolo, S., 1999. Stability of high-Al titanite from low-pressure calc-silicates in light of fluid and host rock composition. Am. Mineral. 84, 37–47.
Meinert, L.D., Dipple, G.M., Nicolescu, S., 2005. World skarn deposits. Economic Geology 100th Anniversary Volume, 299–336.
Moeller, A., O'Brien, P.J., Kennedy, A., Kröner, A., 2003. Linking growth episodes of zircon and metamorphic textures to zircon chemistry: An example from the ultrahigh-temperature granulites of Rogaland (SW Norway). Geol. Soc. Lond. Spec. Publ. 220 (1), 65–81.
Mungall, J.E., 2002. Roasting the mantle: Slab melting and the genesis of major Au and Au-rich Cu deposits. Geology 30, 915–918.
Nakada, S., 1991. Magmatic processes in titanite-bearing dacites, central Andes of Chile and Bolivia. Am. Mineral. 76, 548–560.
Naney, M.T., 1983. Phase equilibria of rock-forming ferromagnesian silicates in gmnitic systems. AM. J. Sci. 283, 993–1033.
Oberti, R., Smith, D.C., Rossi, G., Caucia, F., 1991. The crystal chemistry of high aluminium titanites. Eur. J. Mineral. 3, 777–792.
Pan, Y.M., Dong, P., 1999. The Lower Changjiang (Yangzi/Yangtze River) metallogenic belt, east central China: intrusion- and wall rock-hosted Cu–Fe–Au, Mo, Zn, Pb, Ag deposits. Ore Geol. Rev. 15, 177–242.
Pan, L.C., Hu, R.Z., Bi, X.W., Li, C., Wang, X.S., Zhu, J.J., 2018. Titanite major and trace element compositions as petrogenetic and metallogenic indicators of Mo ore deposits: Examples from four granite plutons in the southern Yidun arc, SW China. Am. Mineral. 103, 1417–1434.
Papapavlou, K., Darling, J.R., Storey, C.D., Lightfoot, P.C., Moser, D.E., Lasallea, S., 2017. Dating shear zones with plastically deformed titanite: New insights into the orogenic evolution of the Sudbury impact structure (Ontario, Canada). Precambrian Res. 291, 220–235.
Peng, H.J., Mao, J.W., Pei, R.F., Zhang, C.Q., Tian, G., Zhou, Y.M., Li, J.X., Hou, L., 2014. Geochronology of the Hongniu-Hongshan porphyry and skarn Cu deposit, northwestern Yunnan province, China: Implications for mineralization of the Zhongdian arc. J. Asian Earth Sci. 79, 682–695.
Qi, L., Hu, J., Gregoire, D.C., 2000. Determination of trace elements in granites by inductively coupled plasma mass spectrometry. Talanta 51, 507–513.
Ribbe, P.H., 1980. Titanite. Rev. Mineral. Geochem. 5, 137–154.
Richards, J.P., 2015. The oxidation state, and sulfur and Cu contents of arc magmas: implications for metallogeny. Lithos 233, 27–45.
Richards, J.P., Kerrich, R., 2007. Special paper: Adakite-like rocks: Their diverse origins and questionable role in metallogenesis. Econ. Geol. 102, 537–576.
Ridolfi, F., Renzulli, A., Puerini, M., 2010. Stability and chemical equilibrium of amphibole in calc-alkaline magmas: an overview, new thermobarometric formulations and application to subduction-related volcanoes. Contrib. Mineral. Petr. 160, 45–66.
Scibiorski, E., Kirkland, C.L., Kemp, A.I.S., Tohver, E., Evans, N.J., 2019. Trace elements in titanite: A potential tool to constrain polygenetic growth processes and timing. Chem. Geol. 509, 1–19.
Shen, P., Hattori, K., Pan, H.D., Jackson, S., Seitmuratova, E., 2015. Oxidation condition and metal fertility of granitic magmas: Zircon trace-element data from porphyry Cu deposits in the Central Asian Orogenic Belt. Econ. Geol. 110, 1861–1878.
Shi, K., Yang, X.Y., Du, J.G., Cao, J.Y., Wan, Q., Cai, Y., 2020. Geochemical study of cretaceous magmatic rocks and related ores of the hucunnan Cu-Mo deposit: Implications for petrogenesis and poly-metal mineralization in the tongling ore-cluster region. Minerals 10. https://doi.org/10.3390/min10020107.
Sun, S.S., McDonough, W.F., 1989. Chemical and isotopic systematics of oceanic basalts: implications for mantle composition and processes. Geochem. Soc. Spec. Publ. 42, 313–345.
Sun, W.D., Xie, Z., Chen, J.F., Zhang, X., Chai, Z.F., Du, A.D., Zhao, J.S., Zhang, C.H., Zhou, T.F., 2003. Os-Os dating of copper and molybdenum deposits along the middle and lower reaches of the Yangtze River, China. Econ. Geol. 98, 175–180.
Sun, W.D., Ding, X., Hu, Y.H., Li, X.H., 2007. The golden transformation of the Cretaceous plate subduction in the west Pacific. Earth. Planet. Sc. Lett. 262, 533–542.
Sun, W.D., Ling, M.X., Yang, X.Y., Fan, W.M., Ding, X., Liang, H.Y., 2010. Ridge subduction and porphyry copper gold mineralization: An overview. Sci. China Earth Sci. 53, 475–484.
Tian, S.H., Ding, T.P., Hou, Z.Q., Yang, Z.S., Xie, Y.L., Wang, Y.B., Wang, X.C., 2005. REE and stable isotope geochemistry of the Xiaotongguanshan copper deposit, Tongling, Anhui. Geol. China 32, 604–613 in Chinese with English abstract.
Tiepolo, M., Oberti, R., Vannucci, R., 2002. Trace element incorporation in titanite: constraints from experimentally determined solid/liquid partition coefficients. Chem. Geol. 191, 105–119.
Troitzsch, U., Ellis, D.J., 2002. Thermodynamic properties and stability of AlF-bearing titanite $CaTiSiO_5$-$CaAlFSiO_4$. Contrib. Mineral. Petr. 142, 543–563.
Vuorinen, J.H., Halenius, U., 2005. Nb-, Zr- and LREE-rich titanite from the Alnö alkaline complex: crystal chemistry and its importance as petrogenetic indicator. Lithos 83, 128–142.
Wang, R., Richards, J.P., Hou, Z.Q., Yang, Z.M., Gu, Z.B., DuFrane, S.A., 2014. Increasing magmatic oxidation state from paleocene to miocene in the Eastern Gangdese Belt, Tibet: implication for collision-related porphyry Cu-Mo±Au mineralization. Econ. Geol. 109, 1943–1965.
Wang, C.S., Wu, C.L., Zheng, K., Wu, D., Shan, S.F., Li, X., Gu, Q.D., 2018. Ore-forming ages and sources of metallogenic materials of Fenghuangshan ore field in Tongling. Mineral Deposits 37, 1195–1216 in Chinese with English abstract.
Wang, Q., Wyman, D.A., Xu, J.F., Zhao, Z.H., Jian, P., Xiong, X.L., Bao, Z.W., Li, C.F., Bai, Z.H., 2006. Petrogenesis of Cretaceous adakitic and shoshonitic igneous rocks in the Luzong area, Anhui Province (eastern China): Implications for geodynamics and Cu-Au mineralization. Lithos 89, 424–446.
Wang, Q., Wyman, D.A., Xu, J.F., Jian, P., Zhao, Z.H., Li, C.F., Xu, W., Ma, J.L., He, B., 2007. Early Cretaceous adakitic granites in the Northern Dabie Complex, central China: Implications for partial melting and delamination of thickened lower crust. Geochim. Cosmochim. Acta 71, 2609–2636.
Wang, R.C., Xie, L., Chen, J., Yu, A.P., Wang, L.B., Lu, J.J., Zhu, J.C., 2011. Titanite as an indicator mineral of tin mineralizing potential of granites in the Middle Nanling Range. Geol. J. China Univ. 17, 368–380 in Chinese with English abstract.
Wang, R.C., Xie, L., Chen, L., Yu, A.P., Wang, L.B., Lu, J.J., Zhu, J.C., 2013. Tin-carrier minerals in metaluminous granites of the western Nanling Range (southern China): Constraints on processes of tin mineralization in oxidized granite. J. Asian Earth Sci. 74, 361–372.
Wang, Y., Yang, X., Deng, J., Liu, S., Sun, C., Hou, Q., Wang, L., 2022. A comprehensive overview on the origin of intrusive rocks and polymetallic mineralization in the Tongling ore-cluster region, lower Yangtze River Metallogenic Belt: Geological and geochemical constraints. Ore Geol. Rev. 141, 104625.
Warner, S., Martin, R.F., Abdel-Rahman, A.-F.-M., Doig, R., 1998. Apatite as a monitor of fractionation, degassing, and metamorphism in the Sudbury igneous complex, Ontario. Can. Mineral. 36, 981–999.
Wu, H.H., Huang, H., Zhang, Z.C., Wang, T., Guo, L., Zhang, Y.H., Wang, W., 2020. Geochronology, geochemistry, mineralogy and metallogenic implications of the Zhaojinggou Nb-Ta deposit in the northern margin of the North China Craton, China. Ore Geol. Rev. 125, 103692.
Xie, J.C., Yang, X.Y., Sun, W.D., 2012. Early Cretaceous dioritic rocks in the Tongling region, eastern China: Implications for the tectonic settings. Lithos 150, 49–61.
Xie, J.C., Wang, Y., Li, Q.Z., Yan, J., Sun, W.D., 2018. Petrogenesis and metallogenic implications of Late Mesozoic intrusive rocks in the Tongling region, eastern China: A case study and perspective review. Int. Geol. Rev. 60, 1361–1380.
Xie, J.C., Tang, D.W., Qian, L., Wang, Y., Sun, W.D., 2020. Geochemistry of sulfide minerals from skarn Cu (Au) deposits in the Fenghuangshan ore field, Tongling, eastern China: Insights into ore-forming process. Ore Geol. Rev. 122, 103537.
Xie, L., Wang, R.C., Chen, J., Zhu, J.C., 2010. Mineralogical evidence for magmatic and hydrothermal processes in the Qitianling oxidized tin-bearing granite (Hunan, South China): EMP and (MC)-LA-ICPMS investigations of three types of titanite. Chem. Geol. 276, 53–68.
Xu, L.L., Bi, X.W., Hu, R.Z., Tang, Y.Y., Wang, X.S., Xu, Y., 2015. LA-ICP-MS mineral chemistry of titanite and the geological implications for exploration of porphyry Cu deposits in the Jinshajiang-Red River alkaline igneous belt, SW China. Miner. Petrol. 109, 181–200.
Xu, X.S., Fan, Q.C., O'Reilly, S.Y., Jiang, S.Y., Griffin, W.L., Wang, R.C., Qiu, J.S., 2005. U-Pb dating of zircons from quartz diorite and its enclaves at Tongguanshan in Anhui and its petrogenetic implication. Chinese Sci. Bull. 49, 2073–2082.

Xu, X., Liu, Z., Fu, Z., Xu, X., Xie, Q., 2019. Petrogenesis of quartz diorite and granodiorite in the Tongling ore district, Anhui Province: Sr-Nd-Hf-O isotopic constraints. Chinese J. Geol. 54, 711–735 in Chinese with English abstract.
Xu, X.C., Lu, S.M., Xie, Q.Q., Bo, L., Chu, G.Z., 2008. SHRIMP zircon U-Pb dating for the magmatic rocks in Shizishan ore-field of Tongling, Anhui Province, and its geological implications. Acta Geol. Sin. 82, 501–509 in Chinese with English abstract.
Xu, J.F., Shinjo, R., Defant, M.J., Wang, Q., Rapp, R.P., 2002. Origin of Mesozoic adakitic intrusive rocks in the Ningzhen area of east China: partial melting of delaminated lower continental crust. Geology 30, 1111–1114.
Yan, J., Chen, J.F., Xu, X.S., 2008. Geochemistry of Cretaceous mafic rocks from the Lower Yangtze region, eastern China: Characteristics and evolution of the lithospheric mantle. J. Asian Earth Sci. 33, 177–193.
Yang, Y.H., Wu, F.Y., Yang, J.H., Chew, D.M., Xie, L.W., Chu, Z.Y., Zhang, Y.B., Huang, C., 2014. Sr and Nd isotopic compositions of apatite reference materials used in U-Th-Pb geochronology. Chem. Geol. 385, 35–55.
Yang, X.N., Xu, Z.W., Lu, X.C., Jiang, S.Y., Ling, H.F., Liu, L.G., Chen, D.Y., 2011. Porphyry and skarn Au-Cu deposits in the Shizishan orefield, Tongling, East China: U-Pb dating and in-situ Hf isotope analysis of zircons and petrogenesis of associated granitoids. Ore Geol. Rev. 43, 182–193.
Yang, M.M., Zhao, F.F., Liu, X.F., Qing, H.R., Chi, G.X., Li, X.Y., Duan, W.J., Lai, C., 2020. Contribution of magma mixing to the formation of porphyry-skarn mineralization in a post-collisional setting: The Machangqing Cu-Mo-(Au) deposit, Sanjiang tectonic belt, SW China. Ore Geol. Rev. 122, 103518.
Zhang, Q., Wang, Y., Qian, Q., 2001. The characteristics and tectonic-metallogenic significances of the adakites in Mesozoic period from eastern China. Acta Petrol. Sinica 17, 236–244 in Chinese with English abstract.
Zhao, X.Y., Yang, Z.S., Zheng, Y.C., Liu, Y.C., Tian, S.H., Fu, Q., 2015. Geology and genesis of the post-collisional porphyry–skarn deposit at Bangpu, Tibet. Ore Geol. Rev. 70, 486–509.
Zheng, Z.J., Du, Y.S., Lu, Y.H., Chen, L.J., Yang, H.M., Zhang, Y., Ren, C.L., Jiang, Y.W., 2015. Fluid mineralization process of Hucunnan Cu-Mo deposit, Tongling, Anhui Province. Mineral Deposits 34, 692–710.
Zhou, X.M., Li, W.X., 2000. Origin of Late Mesozoic igneous rocks in Southeastern China: implications for lithosphere subduction and underplating of mafic magmas. Tectonophysics 326, 269–287.
Zhou, X.M., Sun, T., Shen, W.Z., Shu, L.S., Niu, Y.L., 2006b. Petrogenesis of Mesozoic granitoids and volcanic rocks in South China: a response to tectonic evolution. Episodes 29, 26–33.
Zhou, M.F., Yan, D.P., Wang, C.L., Qi, L., Kennedy, A., 2006a. Subduction-related origin of the 750 Ma Xuelongbao adakitic complex (Sichuan Province, China): Implications for the tectonic setting of the giant Neoproterozoic magmatic event in South China. Earth Planet. Sci. Lett. 248, 286–300.